Coordinated control of senescence by lncRNA and a novel T-box3 co-repressor complex

Pavan Kumar P.[1,2], Uchenna Emechebe[3*], Richard Smith[4*], Sarah Franklin[5], Barry Moore[6], Mark Yandell[6] , Stephen L. Lessnick [1,4,7] and Anne M. Moon[1, 2, 6, 8]

[1] Department of Pediatrics, University of Utah, Salt Lake City, UT 84158

[2]Weis Center for Research, Geisinger Clinic, Danville PA 17822

[3] Department of Neurobiology and Anatomy, University of Utah, Salt Lake City, UT 84112

[4] The Center for Children's Cancer Research at Huntsman Cancer Institute, University of Utah, Salt Lake City, UT 84112

[5]Department of Internal Medicine and the Nora Eccles Harrison Cardiovascular Research & Training Institute, University of Utah, Salt Lake City, UT 84112

[6] Department of Human Genetics, University of Utah, Salt Lake City, UT 84112

[7] Department of Oncological Sciences, Huntsman Cancer Institute, University of Utah, Salt Lake City, UT 84112

*These authors contributed equally to this work.

[8]Corresponding Author:

Anne M. Moon, M.D., Ph.D.
Current address:
Weis Center for Research
100 North Academy Avenue
Danville, PA 17822
570-214-6984
ammoon@geisinger.edu

Keywords: CAPERα, TBX3, p16, RB, UCA1, hnRNPA1, mRNA stability, senescence, oncogenesis, lncRNA, ulnar-mammary syndrome, embryonic development

Running Title: lncRNA UCA1 and CAPERα/TBX3 co-repressor regulate senescence

Abstract

Cellular senescence is a crucial tumor suppressor mechanism. We discovered a CAPERα/TBX3 repressor complex required to prevent senescence in primary cells and mouse embryos. Critical, previously unknown roles for CAPERα in controlling cell proliferation are manifest in an obligatory interaction with TBX3 to regulate chromatin structure and repress transcription of *CDKN2A-p16*^{INK} and the RB pathway. The lncRNA *UCA1* is a direct target of CAPERα/TBX3 repression whose overexpression is sufficient to induce senescence. In proliferating cells, we found that hnRNPA1 binds and destabilizes *CDKN2A-p16*^{INK} mRNA whereas during senescence, *UCA1* sequesters hnRNPA1 and thus stabilizes *CDKN2A-p16*^{INK}. Thus CAPERα/TBX3 and *UCA1* constitute a coordinated, reinforcing mechanism to regulate both *CDKN2A-p16*^{INK} transcription and mRNA stability. Dissociation of the CAPERα/TBX3 co-repressor during oncogenic stress activates *UCA1,* revealing a novel mechanism for oncogene-induced senescence. Our elucidation of CAPERα and *UCA1* functions *in vivo* provides new insights into senescence induction, and the oncogenic and developmental properties of TBX3.

Introduction

Senescence is defined as irreversible arrest of cell growth and loss of replicative capacity [1]. Senescent cells have a large, flattened morphology and a characteristic secretory phenotype. They may be multinucleate, exhibit nuclear distortion, and contain senescence-associated heterochromatin foci (SAHFs) [2]. Senescence can be induced by various stimuli such as DNA damage, metabolic or oxidative stress, or expression of oncoproteins [3-5] .

The p16/retinoblastoma protein (RB) and p53 tumor suppressor pathways are key regulators of senescence induction and maintenance in many cell types [6]. $p14^{ARF}$-p53 activates p21, whereas the $p16^{INK4a}$-RB pathway culminates in E2F transcriptional target repression and senescence [7]. Expression of *CDKN2A-p14^{ARF}* and *CDKN1A-p21^{CIP}* is repressed by the related transcription factors TBX2 and TBX3; this is the postulated mechanism for senescence bypass of *Bmi1*-/- and SV40 transformed mouse embryonic fibroblasts by overexpressed TBX2 and TBX3, respectively [8-10].

Mutations in human *TBX3* cause a constellation of severe birth defects called ulnar-mammary syndrome [11]. Efforts to understand the molecular biogenesis of this developmental disorder uncovered additional functions for TBX3 beyond transcriptional repression [12-14] as well as critical roles in adult tissue homeostasis [15]. The pleiotropic effects of TBX3 gain and loss of function suggest its molecular activities are context and cofactor dependent.

Despite the biologic importance of TBX3, few interacting proteins or target genes have been discovered, and the mechanisms underlying its regulation of cell fate, cell cycle and carcinogenesis are obscure. We found that TBX3 associates with CAPERα

(Coactivator of AP1 and Estrogen Receptor), a protein identified in a liver cirrhosis patient who developed hepatocellular carcinoma [16]. CAPERα regulates hormone responsive expression and alternative splicing of minigene reporters *in vitro* [17,18] but its *in vivo* functions are unknown.

We show that a CAPERα/TBX3 repressor complex is required to prevent premature senescence of primary cells and regulates the activity of core senescence pathways in mouse embryos. We discovered co-regulated targets of this complex *in vivo* and during oncogene-induced senescence (OIS), including a novel tumor suppressor, the lncRNA *UCA1*. *UCA1* is sufficient to induce senescence and does so in part by sequestering hnRNP A1 to specifically stabilize *CDKN2A-p16^{INK}* mRNA. Our finding that CAPERα/TBX3 regulates p16 levels by dual, reinforcing mechanisms position CAPERα/TBX3 and *UCA1* upstream of multiple members of the p16/RB pathway in the regulatory hierarchy that controls cell proliferation, fate and senescence.

Results

CAPERα interacts with TBX3 *in vivo.*

We recently discovered that TBX3 (human) and Tbx3 (mouse) interact with RNA-binding and splicing factors [13]. Among these, mass spectrometry of anti-TBX3 immunoprecipitated (IP'd) proteins identified CAPERα (Figure 1A). Since TBX3 functions in mammary development and may contribute to the pathogenesis of breast and other hormone responsive cancers [19], its interaction with an ERα co-activator drove further investigation.

To determine if Tbx3 and Caperα interact *in vivo*, we IP'd endogenous Caperα from embryonic day (e)10.5 mouse embryo lysates (Fig. 1B). Immunoblotting for Tbx3 confirmed its interaction with Caperα (Fig.1C, lane 5) and *in vitro* pull down assays revealed that their interaction is direct (Fig. 1D, lane 6). *Caperα* is very broadly expressed during mouse embryonic development (Moon, unpublished), whereas *Tbx3* expression is very tissue specific and dynamic. We thus questioned whether the endogenous proteins interact in mouse tissues relevant to malformations seen in humans with UMS. Immunohistochemistry on sectioned e10.5 embryos showed that Tbx3 and Caperα proteins are co-expressed and have distinct localization patterns in different tissues: Caperα is detected in all dorsal root ganglia nuclei (Fig.1E), some of which contain co-localized Tbx3; in proximal limb mesenchyme, Tbx3 and Caperα co-localize in nuclei (Fig.1F) while in some distal cells and the ectoderm, Caperα is nuclear and Tbx3 is cytoplasmic (Fig. 1G, white arrowheads). Such tissue specificity suggests that functions of the Caperα/Tbx3 complex are context dependent.

TBX3 DNA binding and repressor domains (DBD, RD) independently mediate interactions with partner proteins [13,20,21]. To identify domains required for CAPERα interaction, we used a series of overexpression plasmids encoding mouse Tbx3 proteins with different mutations and functional domains (Fig. 1H). The DBD, deleted repressor domain (ΔRD) and exon7 missense mutants are untagged proteins, whereas the C-terminal deletion mutants are Myc-tagged.

In order to assay the interactions of the untagged exogenous proteins with endogenous CAPERα in HEK293 cells, we needed to knockdown endogenous TBX3 with shRNA (Fig. 1I). We previously demonstrated that mutant Tbx3 proteins produced

130 from the overexpression plasmids are present in *TBX3* knockdown HEK293 cells (Fig.
131 S2 in Kumar et al. 2014[13]). CAPERα is present and can be IP'd in the context of
132 knockdown of endogenous *TBX3* and subsequent overexpression of mutant mouse
133 Tbx3 proteins (Fig.1J). Immunoblot of anti-CAPERα IP'd samples shows that the
134 endogenous CAPERα interacts with Tbx3 DBD mutant proteins (Fig. 1J', lanes 2 and 3
135 are L143P and N227D, respectively).
136 The Tbx3 deletion constructs encode Myc- tagged mutants that can be
137 distinguished from endogenous TBX3, so interactions were assayed in wild type
138 HEK293 cells. Myc-tagged deletion mutants are IP'd by the anti-Myc antibody (Fig. 1K),
139 and probing anti-Myc IP'd material for CAPERα reveals that deletions more proximal
140 than amino acid 655 disrupt the CAPERα/Tbx3 interaction (Fig. 1K').
141 The observation that deletions of the Tbx3 C-terminus disrupt the CAPERα/Tbx3
142 interaction led us to test whether the C-terminal repressor domain, which is crucial for
143 the ability of Tbx3 to function as a transcriptional repressor and immortalize fibroblasts
144 [21], plays a role. Although the untagged ΔRD mutant is produced in TBX3 shRNA
145 knockdown cells and IP'd by the anti-Tbx3 antibody (Fig. 1L and [13]) it does not interact
146 with CAPERα (Fig. 1L'). CAPERα also fails to interact with a C-terminal Tbx3
147 frameshift mutant similar to one identified in humans with UMS [22] (Fig. 1, Figure
148 Supplement (FS)1).
149
150 **CAPERα and TBX3 are required to prevent premature senescence of primary**
151 **human and mouse cells.**

Roles for TBX3 in cell cycle regulation and senescence of primary cells have not been reported. We employed loss-of-function to test whether TBX3 is required for sustained proliferation of primary cultured human foreskin fibroblasts (HFFs) and to determine if CAPERα functions in this process. We tested two different CAPERα and TBX3 shRNAs (please see methods for sequences and location in target mRNAs). Both CAPERα and TBX3 shRNAs effectively decreased the amount of CAPERα mRNA (Fig. 2, FS1A and FS2A, B). Knockdown of either protein resulted in a dramatic increase in Senescence Associated β-galatosidase activity (SA-βgal, Fig.2 A-D; Fig.2, FS1 and 2, C-H). This effect is specific because it occurs with 2 different shRNAs and is rescued by overexpression of CAPERα (Fig.2, FS 1B, E, G, H) and Tbx3 (Fig.2 FS2B, E, G, H). For all subsequent experiments, CAPERα shRNA "A" and TBX3 shRNA "A" were used to perform knockdown (KD) in HFFs (protein knockdowns are shown in Fig. 2, FS 1 and FS2, I panels).

The effects of CAPERα and TBX3 KD on HFF cell growth and SA-βgal activity suggest induction of premature senescence. Consistent with this, both KDs dramatically influenced nuclear structure, chromatin organization and formation of SAHFs (Fig. 2G-J). Expression of senescence mediators was increased and conversely, expression of cell growth and cell cycle promoting genes was similarly decreased by CAPERα and TBX3 KD (Fig. 2K-M). Increased expression of *CDKN2A-p16^{INK}* (henceforth referred to as *p16^{INK}*) and decreased *PCNA, E2F1* and *2, CDK2, CDK4, CDC2* transcripts indicate that CAPERα/TBX3 represses the p16/RB pathway in proliferating HFFs. *PMAIP1, CDKN1A-p21,* and other p53 pathway members were also increased. Collectively, these data indicate that CAPERα and TBX3 are required to

prevent senescence of primary HFFs and act upstream of major cell cycle and senescence regulatory pathways.

Tbx3 null murine embryonic fibroblasts undergo p16/RB-mediated premature senescence, Caperα mislocalization and nuclear disruption.

Tbx3 deficiency in mice causes lethal embryonic arrhythmias and limb defects however, these phenotypes are not due to increased apoptosis ([15] and Emechebe and Moon, unpublished). We hypothesized that Tbx3 may prevent senescence of embryonic cells, and so examined murine embryonic fibroblasts (MEFs) from e13.5 wild type (WT) and *Tbx3* null (-/-) embryos. WT MEFS undergo ~ 10 passages with regular, 20 hour doubling times. In contrast, *Tbx3-/-* MEFs had increased SA-βgal activity and ceased proliferating after only 4 passages (Fig.2 N-Q). Most *Tbx3-/-* MEFs had distorted or ruptured nuclei (Fig.2, FS3 A-C) and laminβ1 staining was already altered at passage 1 (Fig.2, FS3 B'). *Caperα* null mutant embryos do not survive long enough to generate MEFs for complementary experiments (Emechebe and Moon, unpublished) however, Caperα localization is markedly abnormal in *Tbx3-/-* MEFS after only 1 passage (Fig.2, FS3 D-F'). These data suggest that Tbx3 is required for preservation of nuclear architecture and to tether Caperα in its normal nuclear domains in proliferating cells.

Consistent with premature senescence seen in *Tbx3* -/- MEFs, key pro-senescence pathways are activated after loss of Tbx3 *in vivo*: in protein lysates from *Tbx3-/-* embryos, RB was hypophosphorylated on multiple serine residues, consistent with increased p16 and decreased Cdk2 and Cdk4 protein levels relative to control (Fig. 2R). The levels of p21 and other senescence markers were increased, while numerous

198 Cyclins and other Cdks were decreased (Fig. 2R, Fig.2, FS3G). All of these findings are
199 consistent with a requirement for Tbx3 to prevent senescence in embryonic mice and
200 MEFs.
201 Previous studies have suggested that overexpression of TBX3 permits
202 senescence bypass by directly repressing *CDKN2A-p14*^{ARF} (*p14*^{ARF}) to activate p53 [9],
203 but a role for TBX3 in regulating *p16*^{INK} and the RB pathway has not been
204 demonstrated. Thus we expected that loss of p53 would rescue senescence resulting
205 from TBX3 or CAPERαKD. To test this, we transduced TBX3 and CAPERα KD HFFs
206 with shRNA to p53 [23] and assayed SA-βgal activity and growth. Surprisingly, although
207 p53 shRNA effectively decreased p53 (Fig.3, FS1 A) it did not rescue SA-βgal activity or
208 growth arrest due to absence of TBX3 or CAPERα (Fig.3 B, E, G, H). In contrast,
209 shRNA-mediated KD of either RB [24] or p16 [25] (Fig. 3, FS1B, C) rescued these
210 phenotypes in TBX3 and CAPERαKD cells (Fig. 3 C, F-H, I-N). These rescue
211 experiments demonstrate that the p16/RB pathway mediates senescence downstream
212 of CAPERα and TBX3 loss-of-function in primary cells.
213
214 **CAPERα/TBX3 regulates chromatin status of the *p16*^{INK} promoter.**
215 Increased p16 protein and RB hypophosphorylation in *Tbx3-/-* embryos and
216 p16/RB- mediated senescence after CAPERα and TBX3 KD could result from loss of
217 direct repression of *p16*^{INK} by CAPERα/TBX3 in proliferating cells. We screened 7
218 amplicons spanning ~6kb upstream of *p16*^{INK} by ChIP-PCR of HFF chromatin (Fig.3,
219 FS2); 3 amplicons were bound by CAPERα and TBX3 (Fig.3O, lanes 7, 10). Loss of
220 either protein decreased the heterochromatic marks H3K9me3 (Fig.3O, lanes 14, 15)

and H3K27me3 (Fig.3, FS3) and increased the euchromatic mark H3K4me3 (Fig. 3O, lanes 17, 18). Notably, less CAPERα occupied *p16^{INK}* elements after TBX3 KD (Fig.3O, lanes 11) while the amount of TBX3 bound post-CAPERα KD was comparable to control (Fig.3O, lanes 9 versus 7). This is consistent with the abnormal localization of CAPERα seen in *Tbx3-/-* MEFS (Fig.2, FS3 D'-F') and indicates that CAPERα requires TBX3 to occupy *p16^{INK}* regulatory chromatin.

We examined whether CAPERα and/or TBX3 associate with promoters of other cell cycle genes that are transcriptionally dysregulated after CAPERα/TBX3 loss-of- function (Fig. 2 K-M). Antibodies against TBX3 and CAPERα ChIP'd the *p14^{ARF}* initiator [26] (Fig.3, FS4 A); here too, TBX3 KD disrupted CAPERα binding (Fig.3, FS4 A', red arrowhead). Neither CAPERα nor TBX3 associated with amplicons scanning 1.8 kb upstream of *CDKN1A-p21* or elements reportedly bound by TBX2 or TBX3 in other cell types (Fig.3, FS4 B) [10,27,28]. Testing for association with known regulatory elements of *CDK2*, *CDK4*, *CDKN1B* was also negative (Fig.3, FS4 C-E)[29-31]. These data indicate that in proliferating primary cells, CAPERα/TBX3 specifically and directly repress the *CDKN2A* locus by binding multiple regulatory sequence elements and regulating chromatin marks.

Expression of the lncRNA *UCA1* is repressed by CAPERα/TBX3 and sufficient to drive senescence of primary cells.

To identify novel genes repressed by CAPERα/TBX3, we employed differential display to detect transcripts that increased in response to KD of TBX3 and CAPERα in HEK293 cells (Fig.4 A-C). Although most transcripts were unaffected by either KD, or

changes were not shared (Fig.4, FS1 A), *DUSP4* and *UCA1* were upregulated (Fig.4D, Fig.4, FS1 B). DUSP4 is known to regulate cell survival and tumor progression, and overexpression induces senescence downstream of RB/E2F [32,33], thus placing CAPERα/TBX3 upstream of another p16/RB effector. Little is known about the function of the lncRNA *UCA1* [34,35], so we investigated it further.

We found that shRNA KD of CAPERα or TBX3 in primary HFFS recapitulated the increase in *UCA1* transcripts seen in HEK293 cells (Fig. 4 E-H). We then tested whether CAPERα/TBX3 directly control transcription of *UCA1* by interacting with potential regulatory elements. Public ChIP data (http://genome.ucsc.edu/) indicate that the 2kb upstream of *UCA1* may contain such elements. We assayed 3 amplicons in this region (Fig. 4I: A1, A2, A3) by ChIP-PCR of TBX3 and CAPERα: only region A3 was bound (Fig. 4J and K, lanes 18, red arrowheads).

We next determined whether increased *UCA1* expression in response to KD of CAPERα or TBX3 was associated with altered chromatin structure (as seen with $p16^{INK}$, Fig. 3O). *UCA1/A3* is normally in a heterochromatin configuration in HFFs, with repressive marks H3K9me3 and H3K27me3 (Fig.4L, lanes 12, 14) and little H3K4me3 (Fig. 4L, lane 18). After TBX3 KD, activating chromatin marks replaced repressive ones (Fig.4L, lanes 13, 15 and 19) and markedly less CAPERα was bound (Fig. 4L, lane 17, red arrowhead). CAPERα KD also led to loss of repressive marks on *UCA1/A3* (Fig.4M lanes 9, 16), although TBX3 remained bound (Fig.4 M, lane 11, red arrowhead). Combined with previous findings, we conclude that: 1) TBX3 recruits CAPERα to *UCA1/A3* chromatin, 2) TBX3 alone is insufficient to repress *UCA1* and, 3) the default state of *UCA1* in proliferating HFFs is repression conferred by CAPERα/TBX3.

UCA1 modulates behavior of bladder cancer cell lines[35] , but there are no data on its function in primary cells; our results suggest that *UCA1* may be involved in premature senescence. *UCA1* transcripts are low in proliferating HFFs, but 4 days after overexpression of *UCA1* (Fig. 5A) a robust SA-βgal response is evident (Fig. 5 B-D). Cells constitutively expressing *UCA1* ceased proliferating during selection and accumulated SAHFs (Fig. 5E, F). Cell proliferation decreased in a *UCA1* dosage-sensitive manner (Fig. 5G-I), consistent with reduced levels of cell cycle promoting transcripts and increased levels of pro-senescence ones (Fig.5J). These transcriptional changes were manifest at the protein level (Fig.5, FS1). Premature senescence resulting from overexpression of *UCA1* in HFFs reveals that this lncRNA is a novel regulator of cell proliferation and may function as a tumor suppressor in some contexts.

Loss of *UCA1* delays the onset of oncogene-induced senescence.

We tested the hypothesis that *UCA1* is required for induction of oncogene-induced senescence (OIS) in primary cells ("RAS": HFFs transduced with constitutively active ^{G12V}RAS[36]). There are markedly more *UCA1* transcripts in RAS compared to presenescent "PS" HFFs (Fig.5K). Knockdown of *UCA1* in RAS HFFs reduced SA-βgal activity (Fig.5L-Q) and improved RAS cell growth: the number of Ki67+ RAS cells was increased at days 3 and 6 after *UCA1* KD (Fig. 5R, P0 and P1). However, by passage 2, the number of Ki67+ cells was not statistically different in *UCA1* KD cells from control, despite persistently low levels of *UCA1* (Fig.5S) and decreased levels of pro-senescence transcripts (Fig.5T). Overall, this indicates that senescence can occur in the

absence of high levels of UCA1 but that timely execution of the OIS program requires *UCA1*.

We next investigated whether increase in *UCA1* transcripts in OIS is a manifestation of loss of CAPERα/TBX3 occupancy/repression of *UCA1/A3*. Indeed, the repressor dissociates from *UCA1/A3* in RAS HFFs and *UCA1/A3* chromatin switches from heterochromatic to euchromatic marks (Fig. 5U). This is consistent with the senescence-inducing effects of CAPERα/TBX3 loss-of-function (Fig. 2) and resulting upregulation of *UCA1* (Fig. 4), and establishes CAPERα/TBX3 regulation of *UCA1* in an independent model of senescence.

UCA1 promotes senescence by sequestering hnRNP A1 to stabilize _p16^{INK}_ mRNA.

Some lncRNAs influence transcription by recruiting chromatin modifiers to target genes [37]. We tested whether the increased levels of prosenescence transcripts occurring in response to *UCA1* (Fig. 5J) were the result activating chromatin changes however, ChIP-PCR assay for H3K9 acetylation of the *p16^{INK}, p14^{ARF}*, *CDKN1A-p21* (and other) promoters did not reveal changes in this activating mark in response to *UCA1* (Fig.5, FS2). We thus tested whether altered mRNA stability contributed to the observed changes. HFFs were transfected with *UCA1* expression or control plasmid and after 2 days, treated with Actinomycin D. Total RNA was collected at 0-4 hours post-treatment and mRNA levels assayed using RT-PCR. Remarkably, overexpression of *UCA1* resulted in the stabilization of mature *p16^{INK}, p14^{ARF}, E2F1* and *TGFβ1* mRNAs: in the time frame examined, *p16^{INK}*, *p14^{ARF}* and *E2F1* mRNAs do not decay and their $t_{1/2}$ values are therefore denoted as “n” (no decay). The half-life estimates

shown were calculated using linear regression; those best fit lines, their equations and R values are shown in Figure 6, Figure Supplement 1. $t_{1/2}$ of *p16*^{INK} mRNA in control cells was 3.9 hours versus n in *UCA1* overexpressing cells; *p14*^{ARF}, 2.4 vs n; *E2F1,* 7.2 vs n; *TGFβ1,* 1.9 vs 2.9. In marked contrast, *MYC, CDKN1A-p21*, *CDKN2D* and *RB* mRNAs decayed at rates indistinguishable from control (Fig. 6A; Fig.6, FS1). The effects of *UCA1* overexpression on *p16*^{INK} mRNA stability were confirmed by Northern blot (Fig.6, FS2).

Regulation of *p16*^{INK} transcript stability is a critical mechanism for growth control [31,38,39] and hnRNP A1 has been postulated to stabilize *p16*^{INK} mRNA [40], but this has not been tested. To this end, we treated HFFs with siRNA to hnRNP A1 and used Actinomycin D to assess stability of *p16*^{INK} transcripts. Loss of hnRNP A1 (Fig. 6, FS 3) stabilized both *p16*^{INK} ($t_{1/2}$ ~ 2.1 in control vs 12.3 after HNRNP A1 knockdown) and *p14*^{ARF} mRNAs ($t_{1/2}$ ~ 1.5 in control vs 6.9 after hnRNP A1 knockdown) but not those of *E2F1* or *MYC* (Fig. 6B). Half-life estimates were obtained as described for panel A and the best fit lines, their equations and R values are shown in Figure 6, Figure Supplement 3B. The differences in control half-lives between Figure 6 A and B are likely attributable to the different treatments used: in A, control cells were transfected with pcDNA3.1 plasmid, while in B, control cells were transfected with control siRNA. The half-life of an mRNA is cell/context specific (as evident in the differences in control half-lives in 6A versus 6B) and in general, cell cycle regulatory genes have short half-lives [41]. The $t_{1/2}$ of *p16*^{INK} mRNA we observed in HFFs transfected with either control plasmid ($t_{1/2}$ ~3.9) or control siRNA ($t_{1/2}$ ~2.1) is similar to that reported in HeLa cells ($t_{1/2}$ ~2.9)[39].

335 The results we obtained were also similar to those reported for *MYC* mRNA [41,42],
336 *CDKN1A* mRNA in HT29-tsp53 cells [43] and ES cells [41], and *E2F1* mRNA in ES cells [41].
337 The half- lives of *Rb* and *TGFβ1* are mRNAs extremely variable and those we obtained
338 in HFFs were shorter than reported in ES cells [41].
339
340 We next used RNA-IP (RIP) to determine if hnRNP A1 binds $p16^{INK}$ and $p14^{ARF}$
341 mRNAs in proliferating cells and found that this was indeed the case (Fig. 6C, lane 6
342 and Fig.6, FS4). Remarkably, hnRNP A1/$p16^{INK}$ binding was lost in RAS HFFs (Fig. 6C,
343 lane 7), despite an overall increase in the number of $p16^{INK}$ transcripts (Fig. 6C, lane 3).
344 As shown previously, *UCA1* RNA levels also increase with RAS (Fig. 6D, lane 3). *UCA1*
345 is bound by hnRNP A1 in PS cells (Fig. 6D, lanes 6, 7; Fig.6, FS5), but unlike $p16^{INK}$,
346 the hnRNP A1/*UCA1* interaction increases in RAS cells (Fig. 6D, lane 7). *TUG1* lncRNA
347 serves as a negative control (Fig. 6E). Protein levels for hnRNP A1 are shown in Fig.
348 6F. The interaction between *UCA1* and hnRNP A1 is specific, as *UCA1* does not bind
349 hnRNP K, C1/C2, H, U, or D (Fig.6, FS5). Although hnRNP A1 binds *MYC* and *p14ARF*
350 mRNAs (Fig. 6, FS4), it does not bind *RB*, *p21* or *CDK6* mRNAs under the numerous
351 conditions tested (Fig.6, FS6).
352 The opposite binding properties of *UCA1* and $p16^{INK}$ mRNA with hnRNP A1 in PS
353 versus RAS HFFs led us to postulate that *UCA1* stabilizes $p16^{INK}$ mRNA during OIS by
354 disrupting the interaction between hnRNP A1 and $p16^{INK}$ mRNA. In control transfected
355 proliferating cells, there is robust binding of $p16^{INK}$ to hnRNP A1 (Fig. 6C, lane13), but
356 direct overexpression of *UCA1* (Fig. 6D, lane 10) or that resulting from TBX3 or
357 CAPERα KD (Fig. 6D, lanes 17,18) disrupts the hnRNP A1/$p16^{INK}$ mRNA interaction

(Fig.6 C, lanes14, 23, 24, red arrowheads). These findings support the hypothesis that loss of hnRNP A1/*p16*^{INK} mRNA interaction in OIS (Fig. 6C, lane 7) is the result of increased *UCA1* expression and its binding and sequestration of hnRNP A1 (Fig. 6D, lane 7). To further test this, we used shRNA to KD *UCA1* in RAS HFFs (Fig. 6D, lane 27). *UCA1* KD restored the interaction between hnRNP A1 and *p16*^{INK} mRNA (Fig. 6C, lane 31) and led to lower levels of total *p16*^{INK} mRNA (Fig. 6C, lane 27), a finding consistent with the negative effects of hnRNP A1/ *p16*^{INK} interaction on stability of *p16*^{INK} transcripts. The effects of *UCA1* on *p16*^{INK} mRNA stability are specific, because hnRNP A1 interactions with *MYC* or *p14*^{ARF} mRNAs are unaffected by *UCA1* (Fig.6, FS1).

In total, these findings indicate that in proliferating cells, the very low quantity of *UCA1* transcripts is insufficient to disrupt hnRNP A1/*p16*^{INK} binding, and levels of *p16*^{INK} mRNA are low due to: 1) direct repression by CAPERα/TBX3 and, 2) *p16*^{INK} mRNA instability conferred by hnRNP A1. When *UCA1* levels increase during OIS, by *UCA1* overexpression, or via KD of CAPERα/TBX3, *UCA1* binds and sequesters hnRNP A1, preventing it from destabilizing *p16*^{INK} mRNA.

The CAPERα/TBX3 co-repressor dissociates during oncogene-induced senescence leading to activation of *UCA1* and pro-senescence pathways.

Increased p16 protein is required for RAS-induced senescence in MEFS and some human cell types [36], leading us to determine whether OIS affects CAPERα/TBX3 occupancy of *p16*^{INK} chromatin. *CDKN2A-p16*^{INK} genomic regulatory elements bound in PS HFFs (Fig.4I) were not occupied by either TBX3 or CAPERα in RAS HFFs (Fig.7A).

Chromatin marks on these regions switched from heterochromatic to euchromatic (Fig. 7B, Fig.7, FS1 A). This was also observed with *UCA1/A3* (Fig. 5U) and *DUSP4* chromatin (Fig.7, FS1 B).

We investigated the possibility that altered quantity of either CAPERα or TBX3 could disrupt the stoichiometry of their interaction and cause dissociation from $p16^{INK}$ and *UCA1* regulatory elements in OIS. Surprisingly, both TBX3 and CAPERα protein levels were increased in RAS HFFs (Fig. 7 C), but they no longer co-IP'd (Fig. 7D, red box). Immunocytochemistry of endogenous TBX3 and CAPERα in PS and RAS HFFs confirmed increased protein levels in OIS (Fig. 7 F-M), and revealed dramatic changes in CAPERα localization: CAPERα immunoreactivity became concentrated in large intranuclear foci (Fig. 7L,M), as we previously observed in early passage *Tbx3-/-* MEFS (Fig.2, FS2 D-F'). These foci are distinct from SAHFs and PML bodies (Fig. 7M and Fig.7, FS2).

To further investigate the molecular basis of senescence initiation after loss of CAPERα/TBX3, we performed genome-wide transcriptional profiling 2 days post CAPERα, TBX3 and control KD in HFFs. More than half of the transcripts with expression altered 1.5 fold or more by CAPERα KD were similarly affected by loss of TBX3 (N=2375 CAPERα KD, 2188 TBX3 KD; 1157 co-regulated, p<<<<0.0001, Fig. 7 Source Data Files 1-3, Fig. 7N,O). Gene ontology-biologic process (GO-BP) analysis with DAVID [44,45] showed highly significant co-regulation of "transcription regulation" (increased expression) and "cell-cycle" (decreased expression) transcripts (Fig. 7N, O). We tested a subset of these with known roles in senescence by qPCR: 100% validated and were similarly altered by RAS (Fig.7, FS3). Further interrogation of this group

revealed that *IL6* and *HDAC9* are CAPERα/TBX3 direct targets and their upregulation in RAS is associated with loss of CAPERα/TBX3 binding (Fig.7, FS4).

We compared CAPERα/TBX3 co-regulated transcripts to a published dataset comparing PS and ^{G12V}RAS fibroblasts [46]. This revealed that 11% of CAPERα/TBX3 up-regulated transcripts were also increased by RAS (Fig. 7N'); among these, GO-BP "programmed cell death" (31%) and "transcription regulation" (34%) were highly overrepresented. 30% of CAPERα/TBX3 down-regulated transcripts were also in the RAS dataset; >1/3 of these were cell cycle genes (Fig. 7O'). In all comparisons, the number of transcripts common to both groups was greater than predicted by chance and highly statistically significant (Fig. 7, Source Data File 3). KEGG pathway analyses revealed overrepresented pathways that were common to both CAPERα/TBX3 and RAS datasets (Fig.7 pie charts, N-O'), but notably fewer pathways were shared in the upregulated group: JAK/STAT, TLR and TGFβ signaling pathways were only significantly overrepresented in the CAPERα/TBX3 dataset.

Discussion

Our knowledge of the regulatory mechanisms that govern the onset and maintenance of senescence in different contexts must be considered fragmentary [37,47]. In this study, we provide compelling evidence for critical and novel functions of CAPERα, the lncRNA *UCA1* and TBX3 in the regulation of cell proliferation and senescence. We have discovered a CAPERα/TBX3 complex that is required to prevent senescence of primary human and mouse cells *in vivo* and that functions as a master regulator of cell proliferation by directly repressing transcription of lncRNA *UCA1*, *p16^{INK}*

427 and other tumor suppressor genes (Fig. 7P). Overexpression of *UCA1* occurs after loss
428 of TBX3/CAPERα and in OIS (Fig.7Q), and is itself sufficient to induce senescence at
429 least in part, by disrupting the interaction of *p16*^{INK} mRNA with hnRNP A1 leading to
430 increased *p16*^{INK} mRNA stability (Fig. 7P,Q). Disrupting the CAPERα/TBX3 complex by
431 decreasing the amount of either TBX3 or CAPERα, or by CAPERα mislocalization
432 during OIS, coordinately increases activity of multiple pro-senescence targets at both
433 the transcriptional and post-transcriptional levels in a reinforcing mechanism.

434 Increased CAPERα has been reported in human breast cancers and a shift
435 from cytoplasmic to nuclear localization correlates with transition from pre-malignant to
436 malignant lesions [48]. In contrast, CAPERα co-activates vRel mediated transcription but
437 inhibits vREL transforming activity *in vitro* [49]. It is likely that anti- or pro- oncogenic
438 activity of CAPERα is determined by cell type and the interacting protein(s) present in a
439 given context; our results suggest that CAPERα has oncogenic potential in primary
440 cells since loss of CAPERα/TBX3 induces premature senescence, a vital tumor
441 suppressor mechanism. CAPERα binds to regulatory chromatin domains via TBX3 but
442 dissociates from these domains and becomes concentrated in large intranuclear foci
443 prior to senescence induced by loss of TBX3 or during OIS. Future efforts will define the
444 composition of CAPER+ nuclear foci and the role of this nuclear subdomain during
445 senescence induction.

446 The TBX3 RD is required for TBX3 to interact with CAPERα (this study),
447 immortalize primary fibroblasts and confer senescence bypass [21]. Since loss of
448 CAPERα activates target gene transcription despite continued TBX3 occupancy, it is

449 the CAPERα/TBX3 complex (interacting via TBX3 RD) that represses pro-senescence
450 target loci. It will be important to determine if previously identified targets of TBX3
451 transcriptional repression are actually regulated by this complex.
452 Additional studies are warranted to determine the precise mechanisms whereby
453 histone status is regulated by CAPERα/TBX3: TBX3 is known to interact directly with
454 HDACs [50], but there are no reports of it or CAPERα interacting with histone
455 methyltransferases or demethylases. Our recently published Mass Spec screen for
456 Tbx3/TBX3 interactors did not identify such factors however, the screen cannot be
457 considered exhaustive as we did not reproducibly detect HDACs or transcription factors
458 previously reported to interact with Tbx3. Future studies to specifically determine
459 whether TBX3 and/or CAPERα interact with, recruit, or modify the function of EZH2,
460 SUV39 and other methyltransferases will be informative.
461 Previous studies showed that TBX3 represses transcription of *p14*^{ARF} (upstream
462 of p53)[11-13], yet embryonic lethality and mammary phenotypes of *Tbx3* mutants are p53-
463 independent [51]. Our findings reconcile these observations because CAPERα/TBX3
464 represses *p16*^{INK}, the p16/RB pathway is activated in *Tbx3-/-* embryos, and knockdown
465 of either RB or p16 (but not p53) prevents senescence after loss of CAPERα/TBX3.
466 Furthermore, *Tbx3-/-* and *Cdk2-/-;Cdk4-/-* mutant embryos share multiple phenotypes
467 including RB hypo-phosphorylation, reduced E2F-target gene expression, decreased
468 proliferation and premature senescence of MEFs [14,52,53]. Our discoveries of multiple
469 CAPERα/TBX3 binding sites across the *CDKN2A* locus, and altered chromatin marks
470 after TBX3 and CAPERα KD, indicate that the complex directly represses transcription
471 by regulating chromatin structure. In total, the data conclusively demonstrate that p16

elevation, *CDK2* and *CDK4* downregulation, and RB hypophosphorylation mediate senescence downstream of CAPERα/TBX3 loss of function in primary human cells and *Tbx3* null mutant embryos. When combined with the pleiotropic effects of CAPERα/TBX3 on *UCA1, DUSP4*, *IL6, HDAC9* and other pathways, it is clear why loss of this repressor induces senescence.

TBX3 may function in nuclear organization and structure: severe changes in nuclear morphology and mislocalization of both CAPERα and laminβ1 are apparent in *Tbx3-/-* MEFs after just one passage, prior to other signs of senescence. Progeria is a rare disease in which *LMNA* mutations induce cellular and organismal senescence in part by altering stoichiometry and interactions of type A and B Lamins. Progeria fibroblasts have decreased expression of *TBX3,* TBX3 interacting proteins, and TBX3 targets [54]. LMNβ1 is a TBX3 interacting protein [13] and expression of *LMNA, LMNβ1* and *LMNβ2* is disrupted by TBX3/CAPERα KD (Fig. 7 Source Data Files 1-3 and Fig. 7 FS3). TBX3 may regulate *LMN* gene expression and physically interact with Lamins to influence nuclear homeostasis.

There are many downregulated genes common to the senescence responses triggered by RAS^{G12V} and loss of CAPERα/TBX3 however, upregulated transcripts and pathways are largely distinct (Fig. 7N'). This is likely attributable to the presence of direct targets of CAPERα/TBX3 repression in the upregulated dataset. It will be informative to determine which Jak-STAT, TLR and TGFβ pathway members (Fig.7N) are direct CAPERα/TBX3 targets, as the complex roles of these pathways in the senescence associated secretory phenotype, inducing or enforcing autocrine and paracrine senescence, and tumor progression are emerging [55-58].

Recent discoveries of the pervasive functions of lncRNAs as "signals, decoys, guides and scaffolds" [47], conferred by their ability to interact with other nucleic acids and as protein ligands, has added new layers of complexity to regulation of transcriptional and post-transcriptional gene expression and translation. Although there has been a logarithmic increase in studies exploring lncRNA expression and activity, potential senescence-regulating activities are still largely unexplored. LncRNA *HOTAIR* functions as a scaffold to regulate ubiquitination of Ataxin-1 and Snurportin-1 to prevent premature senescence [59]. Global alterations in lncRNA expression have been reported in association with replicative senescence [60], and telomere specific lncRNAs that regulate telomere function during this process have been identified [61]. As this manuscript was in revision, regulation of H4K20 trimethylation of rRNA genes by interaction of quiescence -induced lncRNAs *PAPAS* and Suv4-20h2 was reported [62]. To our knowledge, *UCA1* is the first lncRNA sufficient to induce senescence.

UCA1 is expressed in bladder transitional cell carcinomas [34] and influences tumorigenic potential of bladder cancer cell lines [35,63]. A very recent study identified hnRNP I as a *UCA1* interacting protein that stabilizes *UCA1* RNA; this interaction was postulated to decrease translation of p27 to support growth of the MCF7 breast cancer line [64]. In contrast, our results support a tumor suppressor/prosenescence function for *UCA1* in primary cells. *UCA1* increases stability of $p16^{INK}$ mRNA by sequestering hnRNP A1, employing a decoy mechanism that is in some aspects reminiscent of lncRNA *PANDA* sequestering NF-YA transcription factor to prevent activation of proapoptotic p53 targets and promote cell cycle arrest in the DNA damage response [47]. In the case of *UCA1* and hnRNP A1 however, the sequestration has a very specific

effect: even though *UCA1* expression stabilizes (and hnRNP A1 destabilizes) both *p16^{INK}* and *p14^{ARF}* mRNAs (Fig. 6A,B), *UCA1* only disrupts the association of hnRNP A1 with *p16^{INK}* mRNA (Fig. 6C and Fig.6, FS4). In proliferating cells, abundant hnRNP A1 binds with *p16^{INK}* mRNA resulting in *p16^{INK}* degradation. In senescing cells, *p16^{INK}* mRNA levels increase via reinforcing mechanisms of increased transcription and stability: loss of CAPERα/TBX3 activates transcription of *p16^{INK}* and *UCA1,* in turn, *UCA1* sequesters hnRNPA1.

We recognize that the systems we employed (primary HFFs, mouse embryos and MEFs), while very informative models, provide limited information directly applicable to aging or tumorigenesis without further experimentation. Our data support an important role for CAPERα/TBX3 in regulation of senescence in developmental contexts and, since the CAPERα/TBX3 complex regulates known critical tumor suppressors and there is an increasing literature supporting roles for both TBX3 and CAPERα in tumor biology, this is another worthy area for future investigation. As noted above, expression of *CDKN2A-p14^{ARF}* and *CDKN1A-p21^{CIP}* are repressed by TBX2 and TBX3 and this is postulated to confer the ability of overexpressed TBX2 and TBX3 to permit senescence bypass of *Bmi1*-/- and SV40 transformed mouse embryonic fibroblasts, respectively [8-10]. Numerous overexpression studies have suggested a role for TBX3 in breast cancer ([65] and references therein) and recent papers have reported the tumorigenic and proinvasive effects of overexpressed TBX3 in melanoma cells [66,67] which may derive in part from TBX3 repression of E-cadherin expression [68]. More relevant to our work on the importance of the CAPERα/TBX3 complex to prevent senescence and regulate cell proliferation are reports that Tbx3 improves the pluripotency of iPS cells [69] and prevents

differentiation of mouse ES cells [70].

In conclusion, CAPERα/TBX3 acts as a master regulator of cell growth and fate, exerting pleotropic effects by at least two modes of action: 1) regulating chromatin structure and transcription of both coding and non-coding genes and, 2) modulating mRNA stability by altering the association of RNA binding proteins with target transcripts via *UCA1*. Further exploration will identify tissue-specific *UCA1* targets and binding proteins, and determine whether the ability of TBX3 to confer senescence bypass in other contexts requires CAPERα interaction and/or *UCA1* repression. Mining the pathways regulated by *UCA1* and CAPERα/TBX3 will reveal factors that control cell proliferation and fate during development and disease and thus constitute novel cancer therapeutic targets.

Material and Methods

Mass Spectroscopy as in [13]

Protein extraction and immunoprecipitation: Dignam lysates were prepared and incubated for 4 h at 4°C with the appropriate antibody followed by 2 h at 4°C with the pre equilibrated Dynabeads Protein G (Invitrogen). Immune complexes were collected and washed three times with lysis buffer. Pelleted beads were resuspended in 6X Laemmli buffer and subjected to SDS-PAGE analysis followed by immunoblotting with specific antibodies.

Input lanes contain 5% of protein lysate used for IP; the rest was used in the IP and of the IP'd material, 25% was loaded onto the gel for immunoblotting.

Antibodies

Tbx3 [14,15], TBX3 (SC-17871,MAB10089,A303-098A), CAPERα (A300-291A), GST (SC-33613), LaminB1 (SC-56144), C-Myc (SC-40), R-IgG (SC-2027), m-IgG (SC-2025), Anti-Flag (Sigma, F3165), H3K9me3 (Cell Signaling, 9754), H3K4me3 (Cell Signaling, 9751), H3K27me3 (Cell Signaling, 9733), H3K9ace (Cell Signaling, 9649), H4K5ace (Cell Signaling, 9672), H3K14ace (Cell Signaling, 4353), p-RB -Ser 810--811 (SC-16670), p-RB -Ser 795 (SC-7986), p-RB -Ser 780 (SC-12901), Rb1 (SC-73598), H3S10P (SC-8656), H2A K119ub (8240S), p21 (SC-756), p53 (Invitrogen 134100), Cyclin D1 (SC-753), Cyclin D2 (SC-754), Cyclin D3 (SC-755), Cyclin E (SC-20648), CDK2 (SC-6248), CDK4 (SC-601) CDK6 (SC-177), hnRNP K (SC-53620), hnRNP C1/C2 (SC-32308), hnRNP H (SC-10042), hnRNP U (SC-32315), hnRNP A2/B1 (SC-53531), hn RNP A1 (SC-32301), and hnRNP D1 (AB-61193).

MBP pull down assay

Amylose bound MBP and MBP-tagged TBX3 affinity columns were prepared as per the procedure (E8022S, NEB) described in the manufacturer's protocol. These beads were incubated with 5 and 10 µg of GST and GST-CAPER at 4°C for 8 h. Bound proteins were eluted with reduced glutathione and analyzed by Western blotting with anti-CAPER antibody.

Cell transfection

Transfections were performed in HEK293 or EBNA-293 cells with Lipofectamine 2000 (Invitrogen) or in Human fibroblasts with X-tremeGENE HP DNA transfection Reagent (Roche) as per the manufacturer's recommendations.

Plasmids

Wild type Tbx3 and exon 7 missense, deleted repressor domain (Tbx3ΔRD1), and Tbx3ΔNLS were generated by PCR amplification and cloned into pcDNA3.1. C-terminal deletion constructs Tbx3 1-655, Tbx3 1-623, Tbx3 1-565, Tbx3 1-470 were generated by PCR amplification and cloned into pCS2 with an N-terminal Myc tag. Tbx3 L143P and N277D point mutants were kind gifts of Phil Barnett. *UCA1* and CAPERα cDNAs were cloned into pCDN3.1 and PQCXIH for over- expression studies, respectively.

Sequence of all plasmids was confirmed. Tbx3 L143P and N277D point mutants plasmids were kind gifts of Phil Barnett. Wild type CAPERα was generated by PCR amplification and then cloned into pQCXIH retroviral vector; sequence was confirmed. Full length *UCA1* was amplified by PCR and then cloned into pcDNA3.1 vector; sequence was confirmed.

UCA1 Cloning FP: AGTTGCGGCCGCTGACATTCTTCTGGACAATGAG

UCA1 Cloning RP: TCCTGCGGCCGCTTGGCATATTAGCTTTAATGTAG

CAPERα Cloning FP: CATCGCGGCCGCATGGCAGACGATATTGATATTG

CAPERα Cloning RP: ACGTGGATCCTCATCGTCTACTTGGAACCAGTAG

Immunofluroscence

E10.5 embryos were harvested in PBS followed by overnight fixation at 4^0C in 4% paraformaldehyde and processed for 7 μm cryosections. For cell lines, human fibroblasts were cultured on 8-well chamber slides (BD Flacon) and processed for Immunohistochemistry. Immunohistochemistry was performed using primary antibodies listed above and detected using donkey anti- goat or anti-rabbit Alexa fluor 594 (1:500) and goat anti-mouse Alexa fluor 488(1:500) from Invitrogen. Nuclei were stained with Hoechst or DAPI. Slides were imaged with a Nikon ARI inverted confocal microscope at the University of Utah Imaging Core.

Retroviral transduction and selection of stable cells

shRNA oligonucleotides (see sequences below) were annealed and cloned into the pGFP-B-RS, pRFP-C-RS (Origen) vector and PMK0.1 vector. shRNA against luciferase served as a negative control. High-titer retrovirus was produced by transfection of shRNA retroviral construct along with gag/pol and VSVG encoding plasmids into EBNA-293 cells by lipofectamine 2000 reagent as per the manufactures protocol. Virus containing supernatant was collected after 48 hrs of transfection and filtered through 0.45μM filters (Fisher 09-720-4). HEK293 or HFFs were incubated with DMEM

containing polybrene (8mM) and 500 µl of TBX3 or CAPERα shRNA encoding retrovirus. 24 hrs post infection, cells were split to lower densities and blasticidin or puromycin antibiotic selection applied for 2 days. Stably integrated colonies were selected and analyzed for knock down efficiency by western analysis using Tbx3 or CAPERα antibody.

TBX3 shRNA A: targets *TBX3* exon 7
TBX3 shA FP: CCGG GACCATGGAGCCCGAAGAA ttcaagaga
TTCTTCGGGCTCCATGGTC TTTTTG
TBX3 shA RP: AATTCAAAAA GACCATGGAGCCCGAAGAA tctcttgaa
TTCTTCGGGCTCCATGGTC

TBX3 shRNA B: targets *TBX3* exon 5
TBX3 shB FP: CCGG CAGCTCACCCTGCAGTCCA ttcaagaga
TGGACTGCAGGGTGAGCTG TTTTTG
TBX3 shB RP: AATTCAAAAA CAGCTCACCCTGCAGTCCA tctcttgaa
TGGACTGCAGGGTGAGCTG

CAPERα shRNA A: targets *CAPERα* (gene name *RBM39*) exon 5
CAPERα shA FP:
CCGG GACAGAAATTCAAGACGTTttcaagagaAACGTCTTGAATTTCTGTCTTTTTG
CAPER shA RP:
AATTCAAAAA GACAGAAATTCAAGACGTT tctcttgaa AACGTCTTGAATTTCTGTC

CAPERα shRNA B: targets *CAPERα* exon 1
CAPER shB
P:CCGG AAAGCAAGAGCAGAAGTCGTAttcaagagaTACGACTTCTGCTCTTGCTTT TT
TTTG
CAPER shB RP:
AATTCAAAAA AAAGCAAGAGCAGAAGTCGTA tctcttgaa TACGACTTCTGCTCTTGCT
TT

The pMKo.1 puro RB and pMKo.1 puro p53 shRNA vectors were a kind gift of William Hahn obtained via Addgene.
pRB shRNA: Addgene #10670
p53 shRNA: Addgene #10672
p16 shRNA: Addgene #22271
Efficacy and specificity of the pRb, p53, and p16 shRNAs was validated with second shRNAs and these reagents have been used extensively by many investigators in the years since their initial publication [23-25,71-73].

UCA1 shRNA: targets *UCA1* exon 3
UCA1 shA FP:
GATCCGTTAATCCAGGAGACAAAGAtcaagagTCTTTGTCTCCTGGATTAACTTTTTTG
GA
UCA1 shA RP:
AGCTTCCAAAAAAGTTAATCCAGGAGACAAAGActcttgaTCTTTGTCTCCTGGATTAA
CG

Senescence associated β-galactosidase assay
Performed as per the manufacturer's protocol (9860, Cell Signaling).

Population doubling assay/3T5 growth curves (Fig. 2 E, F, R)
Primary HFFs were plated in a 10cm dish and transduced with retrovirus. After 24 hrs, cells were cultured with antibiotic selection (puromycin or blasticidin) for an additional 24-72 hrs. On day 0 of the 3T5 growth curve, cells were trypsinized, counted and 500,000 cells then plated per 10cm dish. This procedure was repeated every 3 days for 15 days. Population doublings were calculated by (logN1/log2)-(logN0/log2) N1=current cell count, N0=Initial cell count. Curves shown in Figure 2 are representative of 2 independent experiments.

Cell count (Fig.5C)

Primary HFFs were plated in 6 well dishes and transfected at 70% confluence. At days noted in the figure, cells were trypsinized and counted using a hemocytometer.

Crystal violet assay/optical density method of cell quantitation

5×10^5 cells were plated per well in 6-well tissue culture plates. At times indicated, medium was removed and cells were washed with PBS, and fixed for 10 minutes in 10% formalin solution. Cells were rinsed 5X with distilled water, and then stained with 100 μl 0.1% crystal violet solution for 30 min., rinsed 5X in water and dried. Cell-associated crystal violet dye was extracted with 500 μl of 10% acetic acid. Aliquots were collected and optical density at 590 nm measured. Each point on the curve shown represents 3 independent plates.

Senescence marker gene expression in TBX3 and CAPERα KD fibroblasts

Primary HFFs were incubated with TBX3 or CAPERα or Control shRNA encoding retrovirus medium with fresh virus added every 8 hrs for 48 hours, followed by antibiotic selection for 6 days. 6 days after selection, floating cells were discarded and adherent cells were utilized for senescence associated β-gal assay or preparation of RNA.

RNA isolation and reverse transcription–PCR analysis.

Total RNA was prepared using the RNeasy RNA isolation kit (Qiagen) or NucleoSpin RNA II Kit (Clontech) and cDNA was synthesized by cDNA EcoDry Premix Double Primed (Clontech) kit. Q-RT-PCR was performed with SoFast Evagreen Supermix (Bio-Rad) as per manufacturer's protocol.

RT-PCR Primer Sequences

TBX3: TGAGGCCTTTGAAGACCATG, TCAGCAGCTATAATGTCCATC

CAPERα: CGGAACAGGCGTTTAGAGAA, TGGCACTGCTCAACTTGTTC

CDK2: GCTTTCTGCCATTCTCATCG, GTCCCCAGAGTCCGAAAGAT

CDK4: ACGGGTGTAAGTGCCATCTG, TGGTGTCGGTGCCTATGGGA

P21: TCAGAGGAGGCGCCATGT, TGTCCACTGGGCCGAAGA

CDC2: GGGGATTCAGAAATTGATCA, TGTCAGAAAGCTACATCTTC

MDM2: ACCTCACAGATTCCAGCTTCG, TTTCATAGTATAAGTGTCTTTTT

MAPK14: TTCTGTTGATCCCACTTCACTGT, ACACACATGCACACACACTAAC

CDKN2C: CAATGGCTCAGTTTTGCTGAATAA, GTAAGATCTGCCTGCCAAAAGC

CDKN2B: AACGGAGTCAACCGTTTCGG, TGTGCGCAGGTACCCTGCA

P16: CAACGCACCGAATAGTTACG, AGCACCACCAGCGTGTC

SerpinE1:CCGGAACAGCCTGAAGAAGTG, GTGTTTCAGCAGGTGGCGC

P14ARF: CCCTCGTGCTGATGCTACTG, ACCTGGTCTTCTAGGAAGCGG

MCM3: CCTTTCCCTCCAGCTCTGTC, CTCCTGGATGGTGATGGTCT

TGFb: AAGGACCTCGGCTGGAAGTG, CCCGGGTTATGCTGGTTGTA

EGR1: CCAGGAGCGATGAACGCAAGCGGCATACCAAG,
GGAGTACGTGGTGGCCACCGACGGGGACCC

E2F1: ATGTTTTCCTGTGCCCTGAG, ATCTGTGGTGAGGGATGAGG

E2F2: GGCCAAGAACAACATCCAGT, TGTCCTCAGTCAGGTGCTTG

IL6R: CATTGCCATTGTTCTGAGGTTC, AGTAGTCTGTATTGCTGATGTC

GSK3b: ACTCCACCGGAGGCAATTG, GCACAAGCTTCCAGTGGTGTT

UCA1:GAAATGGACAACAGTACACGCATATGGGGC,
CCTGTTGCTAAGCCGATGATACATTACCCT

HPRT: GCTGGTGAAAAGGACCTCT, CACAGGACTAGAACACCTGC

PCNA: AAGAGAGTGGAGTGGCTTTTG, TGTCGATAAAGAGGAGGAAGC

CHK2: CTTATGTGGAACCCCCACCTAC, CAGCACGGTTATACCCAGCA

PMAIP1: GTTTTTGCCGAAGATTACCG, CAATGTGCTGAGTTGGCACT

MYC: CTCCCTCCACTCGGAAGGA, GCATTTTCGGTTGTTGCTGAT

CDKN2D: CAACCGCTTCGGCAAGAC, CAGGGTGTCCAGGAATCCA

P53: CCTCACCATCATCACACTGG, TCTGAGTCAGGCCCTTCTGT

RB: TGTGAACATCGAATCATGGAA, TCAGTTGGTGGTTCTCGGTC

CXCL10: GAAATTATTCCTGCAAGCCAATTT, TCACCCTTCTTTTTCATGTAGCA

IFNB1: GAATGGGAGGCTTGAATACTGCCT, TAGCAAAGATGTTCTGGAGCATCTC

ATF3: GTTTGAGGATTTTGCTAACCTGAC, AGCTGCAATCTTATTTCTTTCTCGT

DUSP2: GGCCTTTGACTTCGTTAAGC, CCACCTCAGTGACACAGCAC

CREB5: CGTGCCTCCTTGAAACAAGCCATT, ATGAAACACCAGCACCTGCCTAGA

HDAC9: AGTGTGAGACGCAGACGCTTAG, TTTGCTGTCGCATTTGTTCTTT

SP140: TGGGTCAGTTTCTTGTTTATCTGC, AGCAGGCTAGAAGCAAGCTC

EGR2: TTGGTGCCTTGTGTGATGTAGAC, CTTTCCATAAGGCAACCCATTT

HMGA2: GTCCCTCTAAAGCAGCTCAAAA, CTCCCTTCAAAAGATCCAACTG

BIRC5: CATGGTAGGTGCAGGTGATG, CATGGTAGGTGCAGGTGATG

ASF1: GGTTCGAGATCAGCTTCGAG, CATGGTAGGTGCAGGTGATG

WDR66: CCGAGAAGCAACAGGAGAAA, CTGTGTCTCCAAACGGATCA

CDC25C: GACACCCAGAAGAGAATAATCATC, CGACACCTCAGCAACTCAG

CENPF: CGAAGAACAACCATGGCAACTCG, TTCTCGGAGGATGGTGCCTGAAT

LAMA2: AATTTACCTCCGCTCGCTAT, CCTCCAATGTACTTTCCACG

LMNB1: AAGCAGCTGGAGTGGTTGTT, TTGGATGCTCTTGGGGTTC

LMNB2: GCTCTGACCAGAACGACAAGG, CCAGCATCTTCCGGAACTTG

CDC20: TCCAAGGTTCAGACCACTCC, GATCCAGGCCACAGACCATA

DUSP5: GCTCGCTCAACGTCAACCTCAACTCGGTG,
AGTGGCGGCTGCCCTGGTCCAGCACCACC

DUSP4: CCTGGCAGCCATCCCACCCCCGGTTCCCC,
GCTGATGCCCAGGGCGTCCAGCATGTCTCTC

mTbx3: TGAGGCCTCTGAAGACCATG, TCAGCAGCTATAATGTCCATC

mSerpinE1: AGCCAACAAGAGCCAATCAC, GGATTCTCGGAGGGGTAAAG

mIL6: GATGGATGCTACCAAACTGGA, CCAGGTAGCTATGGTACTCCAGAA

mP21: TCCACAGCGATATCCAGACA, GGCACACTTTGCTCCTGTG

mCdc2: CTGCAATTCGGGAAATCTCT, TCCATGGACAGGAACTCAAA

mReprimo: CTTACGGACCTGGGACTTTG, CCAGCACTGAATTCATCACG

MEF isolation from WT and *Tbx3* null embryos

All steps were performed under aseptic conditions. Pregnant female mice were euthanized and 13.5 days old embryos were isolated from the uterus. Embryos were washed in sterile PBS in 60-mm tissue culture dish at room temperature and transferred into 15ml sterile falcon tube containing 1 ml of 50% trypsin in DMEM medium. Embryos were minced using fine scissors followed by gentle pipetting with 1ml pipette tips and dispersed into cell suspensions in 5 mins. Suspensions were plated into 10cm plates in 10ml of DMEM with 5% FBS and penicillin/streptomycin and incubated for 8hrs in CO2 incubator. Culture medium was replaced with fresh medium every day for three days. Passage 0 refers to the stage when cell suspension from the embryos was put into cell culture and subsequent passages are numbered.

Chromatin Immunoprecipitation (ChIP)

Performed as per the manufacturer's protocol (9003S, Cell Signaling).

ChIP Primers

UCA1 FP1: GGCTCTCGAGTCAAGATAATTCACTTAC,

UCA1 RP1: GGCACATCTTTGTTGTCTGAAAGGGAT

UCA1 FP2: CACCTCTTTCTTGCCTCCTTGGATATATT,

UCA1 RP2: CACTTACTTACTTATAATAGAGTCAGGGTCT

UCA1 FP3: CCAGGAGCTGATATTCATGACCCTCCA,

UCA1 RP3: CTTGGCTCCTGTAGGCCACCTGGACAT

DUSP4 FP: CGAGGGCACCGGTACCCGCCGGGTCTCTCC

DUSP4 RP: GGACTAGGGTGAGCACAAGCCTTGAGCGC

P16 1A FP: CGACCGTAACTATTCGGTGCGTTGGGCAGC

P16 1A RP: GCTCTGGCGAGGGCTGCTTCCGGCTGGTGC

P16 2A FP: GAGCAGGACGCGGTGGCTCACACCTGTAAT

P16 2A RP: CAGGCATGCGCCACCAAGCCCCGCTAATT

P16 3A FP: CCTCGGGGTACCTCTCAATTAGCTGTGTA

P16 3A RP: AGTTCGAGACAAGCCTAGCCAACATAGTG

P16 4A FP: GAAACTCTACCATGGATTCCTACATCAAG

P16 4A RP: GCACAATGTGCAGGTTTGTTACATATGTAT

P16 5A FP: CCAGTCTCAGATTTCCTATGTGCAAAATG

P16 5A RP: GGTTTGAACCCTGGCAGTCTGACTGTAG

P16 6A FP: GCGGTGGTTATAGATTTTGTCACAAGAG

P16 6A RP: ACTCTGGAACACTACCTTCTCAAGTATC

P16 7A FP: ACCCCGATTCAATTTGGCAG

P16 7A RP: AAAAAGAAATCCGCCCCCG

P14ARF: FP: GCCGAATCCGGAGGGTCACCAAGAACCTGC

P14ARF: RP: GTGCGCAGGGCTCAGAGCCGTTCCGAGATCT

CDK2 FP: GATGGAACGCAGTATACCTCTC;

CDK2 RP: AAAGCAGGTACTTGGGAAGAGTG

CDK4 FP: GTGGACCGAAAAGGTGACAGGATC

CDK4 RP: GGGCGGGGCGAACGCCGGACGTTC

P21 −324 to −676 FP: CCCGGAAGCATGTGACAATC

P21 −324 to −676 RP: CAGCACTGTTAGAATGAGCC

P21 −677 to −981 FP: GGAGGCAAAAGTCCTGTGTTC

P21 −677 to −981 RP: GGAAGGAGGGAATTGGAGAG

P21 −964 to −1340 FP: CTGAGCAGCCTGAGATGTCAG

P21 −964 to −1340 RP: CACAGGACTTTTGCCTCCTG

P21 −1335 to −1688 FP: GAAATGCCTGAAAGCAGAGG

P21 −1335 to −1688 RP: GCTCAGAGTCTGGAAATCTC

CDKN1B FP: CGGCCGTTTGGCTAGTTTGTTTGT

CDKN1B RP: GGAGGCTGACGAAGAAGAAGATGA

HDAC9CHIPFP: GGCTCAGGCCGACCATTGTTCTATTTCTGT

HDAC9CHIPRP: CCTGAGGAGAAGCAGCAGAGGATCAAC

IL6CHIPFP: GAACCAAGTGGGCTTCAGTAATTTCAGG

IL6CHIPRP: CATCTGAGTTCTTCTGTGTTCTGGCTCTC

P14ARF FP: CCCTCGTGCTGATGCTACTG

P14ARF RP: ACCTGGTCTTCTAGGAAGCGG

TGFB1 FP: GATGGCACAGTGGTCAAGAGC

TGFB1 RP: GAAGGATGGAAGGGTCAGGAG

RB FP: GGCGGAAGTGACGTTTTC

RB RP: CCGACTCCCGTTACAAAAAT

MYC FP: AAGATCCTCTCTCGCTAATCTCC

MYC RP: AGAAGCCCTGCCCTTCTC

E2F1 FP: GGCTACAGGTGAGGGTCACG

E2F1 RP: GAGCGCCGCCACAATTGGCT

CDKN2D FP: TCCCTTTCTTCACGGTGCTT

CDKN2D RP: GCGTCGCTCCTGATTGGTC

CDK2 FP : AAGCAGGTACTTGGGAAGAGTGTTCAGC

CDK2 RP: CAACTTGAAACAATGTTGCCGCCTCC

MDM2 FP: GGCCTACCCAAAGTGATGGGATTACAAG

MDM2 RP: GCCGCTGGAGTTGTACCCAAATGAGTTA

<u>siRNA knockdown</u>

For differential display (Figure 4), HEK293 cells were transfected with control siRNAs (Sense; 5' CAGCGACUAAACACAUCA-3' Antisense; 5'-UUGAUGUGUUUAGUCGCUGTT-3') or TBX3 specific siRNA A (Sense: GACCAUGGAGCCCGAAGAA, Antisense: UUCUUCGGGCUCCAUGGU) or CAPERα specific siRNA (Sense: GACAGAAAUUCAAGACGUU, Antisense: AACGUCUUGAAUUUCUGUC) using lipofectamine 2000 (Invitrogen) or X-treme GENE HP DNA transfection reagent as per manufacturer's instructions.

HNRNP A1 siRNA for knockdown in HFFs (Figure 6) was obtained from Cell Signaling (cat. #7668).

<u>Oncogene-induced senescence with constituitively active RAS.</u>

^{V12G}RAS virus was produced with pBABE-^{V12G}RAS as per the procedure described above. HFFs were transduced with RAS virus and incubated with antibiotic selection medium (puromycin 2 μg/ml) for 4-5 days.

RNA immunoprecipitation (RIP) and RIP-PCR

For RNA Immunoprecipitation, 10 million cells were lysed in 1 ml of NP-40 lysis buffer (50mM Tris HCl, ph7.4, 150 mM NaCl, 1% NP-40 and Protease inhibitor cocktail). Lysate was cleared by centrifugation at 12000 RCF for 15 mins. Cleared lysate was immunoprecipitated independently with 5 μg of anti-hnRNP A1, anti-hnRNP D, Anti-hnRNP A2/B1, Anti-hnRNP C1/C2, Anti-hnRNP K, mIgG and R-IgG antibodies. Immune complexes were incubated with 30 μL of pre-equilibrated Dynabeads for 4 hrs at 4^0C. Dynabead purified immune complexes were subjected to Proteinase K digestion at 37°C for 1 hr followed by NucleoSpin RNA II purification kit and cDNA was prepared by RNA-to-cDNA EcoDry Premix kit (Clontech). cDNA was used as a template in PCR amplifications with gene specific primers.

mRNA stability assays

TBX3, CAPERα or Control shRNA KD, PS and RAS HFFs were cultured in 6 well culture dishes for 2 days to 80% confluence. Then Actinomycin D was added to a final concentration of 5 mg/ml to suppress transcription. At 0, 1, 2 and 4 hours after addition of Actinomycin D, equal numbers of cells were harvested from each sample and mRNA was prepared by nucleoSpin RNA II purification kit and cDNA was prepared by RNA-to-cDNA EcoDry Premix kit (Clontech) followed by qRT-PCR for specific transcripts.

$P16^{INK}$ mRNA Northern blot

HFFs were transfected with pcDNA3.1 control or *UCA1* expression plasmids as described above, incubated +/- Actinomycin D, and total cellular RNA was harvested at 0, 1, 2 and 4 hrs post treatment. For northern blot analysis, 5 μg total RNA from each time point was electrophoresed through a 1% agarose gel. The RNA was blotted onto Hybond-N+ membrane (Amersham Pharmacia), and membranes were UV crosslinked. Membranes were hybridized for 18 hrs with ^{32}P-labeled probes. Probes were generated by end-labeling DNA oligonucleotides containing following sequences complementary to *$p16^{INK}$* mRNA:

1) 5’ GAGGAGGTGCTATTAACTCCGAGCATTAGCGAATGTGGC

2) 5’ AATCCTCTGGAGGGACCGCGGTATCTTTCCAGGCAAGGGG

3) 5’AAGGCTCCATGCTGCTCCCCGCCGCCGGCTCCATGCTGCT

End-labeling reactions were performed using T4 polynucleotide Kinase (NEB) according to the manufacturer’s directions. The hybridized blots were washed, and autoradiographs were developed as per standard procedure. Band intensities were measured by Image J analysis and densitometric vales were plotted as bar graphs.

RNA-Seq analysis of TBX3 and CAPERα KD HFFs

HFFs were incubated with TBX3 or CAPER α shRNA encoding retrovirus for 48 hours followed by incubation for an additional 48 hours in selection medium. Total RNA was isolated and purity was assessed. Poly-A RNA was purified, fragmented, primed with random hexamers and used to generate first strand cDNA using reverse transcriptase. Samples that passed quality control steps were used for Illumina library preparation using the Illumina TruSeq RNA Sample Prep protocol. All libraries were sequenced (with barcoding) on a single lane of an Illumina HiSeq instrument for 50 cycles from a single end. A total of 177,155,781 reads were produced in total for all 10 libraries (median 17,348,374 reads). Base calling was performed using Illumina software.

Bioinformatics analysis

Sequence reads were aligned (98.5% mapped) to the human genome build 37.2 with Tophat (v2.0.8b) using default parameters. Aligned reads were assembled into transcripts and their relative abundance was measured using Cufflinks (v2.1.1) with fragment bias correction (frag-bias-correct) and multi-read correction (multi-read-correct). Cufflinks transcript assemblies were based on transcripts of NCBI Homo sapiens annotation release 104 and miRBase release 19 as provided in the Illumina iGenomes dataset. Cuffdiff was used to test for differential expression between samples and controls and expression differences were taken as significant if the FDR adjusted p-value was less than 0.05 (Source Data Files 1 and 2). Statistically

overrepresented gene ontology/biologic process categories and KEGG pathways were determined using DAVID [44,45]. The hypergeometric test, as implemented in the R statistical language (phyper), was used to test significance of the number of genes found to be co-regulated between samples (Source Data File 3).

Acknowledgements

We thank J. Michael Dean and Thomas Vondriska for their support of Drs. Kumar and Franklin, respectively. We thank Nikos Tapinos, David Carey, Alana Welm, Kirk Thomas and Ashley Firment for critical reading of the manuscript. Phillip Barnett kindly provided the Tbx3 DBD mutant plasmids.

References

1. Hayflick, L. The Limited in Vitro Lifetime of Human Diploid Cell Strains. *Exp Cell Res* **37**, 614-36 (1965).
2. Kosar, M. et al. Senescence-associated heterochromatin foci are dispensable for cellular senescence, occur in a cell type- and insult-dependent manner and follow expression of p16(ink4a). *Cell Cycle* **10**, 457-68 (2011).
3. Coppe, J.P. et al. Tumor suppressor and aging biomarker p16(INK4a) induces cellular senescence without the associated inflammatory secretory phenotype. *J Biol Chem* **286**, 36396-403 (2011).
4. Kuilman, T., Michaloglou, C., Mooi, W.J. & Peeper, D.S. The essence of senescence. *Genes Dev* **24**, 2463-79 (2010).
5. Larsson, O. Cellular senescence- an integrated perspective. *Cancer Therapy* **3**, 495-510 (2005).
6. Narita, M. et al. Rb-mediated heterochromatin formation and silencing of E2F target genes during cellular senescence. *Cell* **113**, 703-16 (2003).
7. DeGregori, J. The Rb network. *J Cell Sci* **117**, 3411-3 (2004).
8. Jacobs, J.J. et al. Senescence bypass screen identifies TBX2, which represses Cdkn2a (p19(ARF)) and is amplified in a subset of human breast cancers. *Nat Genet* **26**, 291-9 (2000).
9. Brummelkamp, T.R. et al. TBX-3, the gene mutated in Ulnar-Mammary Syndrome, is a negative regulator of p19ARF and inhibits senescence. *J Biol Chem* **277**, 6567-72 (2002).
10. Prince, S., Carreira, S., Vance, K.W., Abrahams, A. & Goding, C.R. Tbx2 directly represses the expression of the p21(WAF1) cyclin-dependent kinase inhibitor. *Cancer Res* **64**, 1669-74 (2004).
11. Bamshad, M. et al. Mutations in human TBX3 alter limb, apocrine and genital development in Ulnar-Mammary Syndrome. *Nature Genetics* **16**, 311-315 (1997).

12. Fan, C., Chen, Q. & Wang, Q.K. Functional role of transcriptional factor TBX5 in pre-mRNA splicing and Holt-Oram syndrome via association with SC35. *J Biol Chem* **284**, 25653-63 (2009).
13. Kumar, P.P. et al. TBX3 Regulates Splicing In Vivo: A Novel Molecular Mechanism for Ulnar-Mammary Syndrome. *PLoS Genet* **10**, e1004247 (2014).
14. Frank, D.U., Emechebe, U., Thomas, K.R. & Moon, A.M. Mouse tbx3 mutants suggest novel molecular mechanisms for ulnar-mammary syndrome. *PLoS One* **8**, e67841 (2013).
15. Frank, D.U. et al. Lethal arrhythmias in Tbx3-deficient mice reveal extreme dosage sensitivity of cardiac conduction system function and homeostasis. *Proc Natl Acad Sci U S A* (2012).
16. Imai, H., Chan, E.K., Kiyosawa, K., Fu, X.D. & Tan, E.M. Novel nuclear autoantigen with splicing factor motifs identified with antibody from hepatocellular carcinoma. *J Clin Invest* **92**, 2419-26 (1993).
17. Jung, D.J., Na, S.Y., Na, D.S. & Lee, J.W. Molecular cloning and characterization of CAPER, a novel coactivator of activating protein-1 and estrogen receptors. *J Biol Chem* **277**, 1229-34 (2002).
18. Dowhan, D.H. et al. Steroid hormone receptor coactivation and alternative RNA splicing by U2AF65-related proteins CAPERalpha and CAPERbeta. *Mol Cell* **17**, 429-39 (2005).
19. Douglas, N.C. & Papaioannou, V.E. The T-box Transcription Factors TBX2 and TBX3 in Mammary Gland Development and Breast Cancer. *J Mammary Gland Biol Neoplasia* **18**, 143-7 (2013).
20. Coll, M., Seidman, J.G. & Muller, C.W. Structure of the DNA-bound T-box domain of human TBX3, a transcription factor responsible for ulnar-mammary syndrome. *Structure* **10**, 343-56 (2002).
21. Carlson, H., Ota, S., Campbell, C.E. & Hurlin, P.J. A dominant repression domain in Tbx3 mediates transcriptional repression and cell immortalization: relevance to mutations in Tbx3 that cause ulnar-mammary syndrome. *Hum Mol Genet* **10**, 2403-13 (2001).
22. Bamshad, M. et al. The spectrum of mutations in TBX3: genotype/pheotype relationship in Ulnar-Mammary Syndrome. *Am. J. Hum. Genet.* **64**, 1550-1562 (1999).
23. Masutomi, K. et al. Telomerase maintains telomere structure in normal human cells. *Cell* **114**, 241-53 (2003).
24. Boehm, J.S., Hession, M.T., Bulmer, S.E. & Hahn, W.C. Transformation of human and murine fibroblasts without viral oncoproteins. *Mol Cell Biol* **25**, 6464-74 (2005).
25. Haga, K. et al. Efficient immortalization of primary human cells by p16INK4a-specific short hairpin RNA or Bmi-1, combined with introduction of hTERT. *Cancer Sci* **98**, 147-54 (2007).
26. Lingbeek, M.E., Jacobs, J.J. & van Lohuizen, M. The T-box repressors TBX2 and TBX3 specifically regulate the tumor suppressor gene p14ARF via a variant T-site in the initiator. *J Biol Chem* **277**, 26120-7 (2002).
27. Hoogaars, W.M. et al. TBX3 and its splice variant TBX3 + exon 2a are functionally similar. *Pigment Cell Melanoma Res* **21**, 379-87 (2008).

28. Saramaki, A., Banwell, C.M., Campbell, M.J. & Carlberg, C. Regulation of the human p21(waf1/cip1) gene promoter via multiple binding sites for p53 and the vitamin D3 receptor. *Nucleic Acids Res* **34**, 543-54 (2006).
29. Louie, M.C., McClellan, A., Siewit, C. & Kawabata, L. Estrogen receptor regulates E2F1 expression to mediate tamoxifen resistance. *Mol Cancer Res* **8**, 343-52 (2010).
30. Baksh, S. et al. NFATc2-mediated repression of cyclin-dependent kinase 4 expression. *Mol Cell* **10**, 1071-81 (2002).
31. Wang, C. et al. Activation of p27Kip1 Expression by E2F1. A negative feedback mechanism. *J Biol Chem* **280**, 12339-43 (2005).
32. Torres, C., Francis, M.K., Lorenzini, A., Tresini, M. & Cristofalo, V.J. Metabolic stabilization of MAP kinase phosphatase-2 in senescence of human fibroblasts. *Exp Cell Res* **290**, 195-206 (2003).
33. Wang, J., Shen, W.H., Jin, Y.J., Brandt-Rauf, P.W. & Yin, Y. A molecular link between E2F-1 and the MAPK cascade. *J Biol Chem* **282**, 18521-31 (2007).
34. Wang, X.S. et al. Rapid identification of UCA1 as a very sensitive and specific unique marker for human bladder carcinoma. *Clin Cancer Res* **12**, 4851-8 (2006).
35. Wang, F., Li, X., Xie, X., Zhao, L. & Chen, W. UCA1, a non-protein-coding RNA up-regulated in bladder carcinoma and embryo, influencing cell growth and promoting invasion. *FEBS Lett* **582**, 1919-27 (2008).
36. Serrano, M., Lin, A.W., McCurrach, M.E., Beach, D. & Lowe, S.W. Oncogenic ras provokes premature cell senescence associated with accumulation of p53 and p16INK4a. *Cell* **88**, 593-602 (1997).
37. Fatica, A. & Bozzoni, I. Long non-coding RNAs: new players in cell differentiation and development. *Nat Rev Genet* **15**, 7-21 (2014).
38. Zhang, X. et al. The tRNA methyltransferase NSun2 stabilizes p16INK(4) mRNA by methylating the 3'-untranslated region of p16. *Nat Commun* **3**, 712 (2012).
39. Chang, N. et al. HuR uses AUF1 as a cofactor to promote p16INK4 mRNA decay. *Mol Cell Biol* **30**, 3875-86 (2010).
40. Zhu, D., Xu, G., Ghandhi, S. & Hubbard, K. Modulation of the expression of p16INK4a and p14ARF by hnRNP A1 and A2 RNA binding proteins: implications for cellular senescence. *J Cell Physiol* **193**, 19-25 (2002).
41. Sharova, L.V. et al. Database for mRNA half-life of 19 977 genes obtained by DNA microarray analysis of pluripotent and differentiating mouse embryonic stem cells. *DNA Res* **16**, 45-58 (2009).
42. Herrick, D.J. & Ross, J. The half-life of c-myc mRNA in growing and serum-stimulated cells: influence of the coding and 3' untranslated regions and role of ribosome translocation. *Mol Cell Biol* **14**, 2119-28 (1994).
43. Melanson, B.D. et al. The role of mRNA decay in p53-induced gene expression. *RNA* **17**, 2222-34 (2011).
44. Huang da, W., Sherman, B.T. & Lempicki, R.A. Systematic and integrative analysis of large gene lists using DAVID bioinformatics resources. *Nat Protoc* **4**, 44-57 (2009).

45. Huang da, W., Sherman, B.T. & Lempicki, R.A. Bioinformatics enrichment tools: paths toward the comprehensive functional analysis of large gene lists. *Nucleic Acids Res* **37**, 1-13 (2009).
46. Loayza-Puch, F. et al. p53 induces transcriptional and translational programs to suppress cell proliferation and growth. *Genome Biol* **14**, R32 (2013).
47. Wang, K.C. & Chang, H.Y. Molecular mechanisms of long noncoding RNAs. *Mol Cell* **43**, 904-14 (2011).
48. Mercier, I. et al. Genetic ablation of caveolin-1 drives estrogen-hypersensitivity and the development of DCIS-like mammary lesions. *Am J Pathol* **174**, 1172-90 (2009).
49. Dutta, J., Fan, G. & Gelinas, C. CAPERalpha is a novel Rel-TAD-interacting factor that inhibits lymphocyte transformation by the potent Rel/NF-kappaB oncoprotein v-Rel. *J Virol* **82**, 10792-802 (2008).
50. Yarosh, W. et al. TBX3 is overexpressed in breast cancer and represses p14 ARF by interacting with histone deacetylases. *Cancer Res* **68**, 693-9 (2008).
51. Jerome-Majewska, L.A. et al. Tbx3, the ulnar-mammary syndrome gene, and Tbx2 interact in mammary gland development through a p19Arf/p53-independent pathway. *Dev Dyn* **234**, 922-33 (2005).
52. Frank, D.U. et al. Lethal arrhythmias in Tbx3-deficient mice reveal extreme dosage sensitivity of cardiac conduction system function and homeostasis. *Proc Natl Acad Sci U S A* **109**, E154-63 (2012).
53. Berthet, C. et al. Combined loss of Cdk2 and Cdk4 results in embryonic lethality and Rb hypophosphorylation. *Dev Cell* **10**, 563-73 (2006).
54. Csoka, A.B. et al. Genome-scale expression profiling of Hutchinson-Gilford progeria syndrome reveals widespread transcriptional misregulation leading to mesodermal/mesenchymal defects and accelerated atherosclerosis. *Aging Cell* **3**, 235-43 (2004).
55. Davalos, A.R. et al. p53-dependent release of Alarmin HMGB1 is a central mediator of senescent phenotypes. *J Cell Biol* **201**, 613-29 (2013).
56. Senturk, S. et al. Transforming growth factor-beta induces senescence in hepatocellular carcinoma cells and inhibits tumor growth. *Hepatology* **52**, 966-74 (2010).
57. Hubackova, S., Krejcikova, K., Bartek, J. & Hodny, Z. IL1- and TGFbeta-Nox4 signaling, oxidative stress and DNA damage response are shared features of replicative, oncogene-induced, and drug-induced paracrine 'bystander senescence'. *Aging (Albany NY)* **4**, 932-51 (2012).
58. Hubackova, S. et al. Regulation of the PML tumor suppressor in drug-induced senescence of human normal and cancer cells by JAK/STAT-mediated signaling. *Cell Cycle* **9**, 3085-99 (2010).
59. Yoon, J.H. et al. Scaffold function of long non-coding RNA HOTAIR in protein ubiquitination. *Nat Commun* **4**, 2939 (2013).
60. Abdelmohsen, K. et al. Senescence-associated lncRNAs: senescence-associated long noncoding RNAs. *Aging Cell* **12**, 890-900 (2013).
61. Yu, T.Y., Kao, Y.W. & Lin, J.J. Telomeric transcripts stimulate telomere recombination to suppress senescence in cells lacking telomerase. *Proc Natl Acad Sci U S A* **111**, 3377-82 (2014).

62. Bierhoff, H. et al. Quiescence-Induced LncRNAs Trigger H4K20 Trimethylation and Transcriptional Silencing. *Mol Cell* (2014).
63. Yang, C., Li, X., Wang, Y., Zhao, L. & Chen, W. Long non-coding RNA UCA1 regulated cell cycle distribution via CREB through PI3-K dependent pathway in bladder carcinoma cells. *Gene* **496**, 8-16 (2012).
64. Huang, J. et al. Long non-coding RNA UCA1 promotes breast tumor growth by suppression of p27 (Kip1). *Cell Death Dis* **5**, e1008 (2014).
65. Liu, J. et al. TBX3 over-expression causes mammary gland hyperplasia and increases mammary stem-like cells in an inducible transgenic mouse model. *BMC Dev Biol* **11**, 65 (2011).
66. Peres, J. et al. The Highly Homologous T-Box Transcription Factors, TBX2 and TBX3, Have Distinct Roles in the Oncogenic Process. *Genes Cancer* **1**, 272-82 (2010).
67. Peres, J. & Prince, S. The T-box transcription factor, TBX3, is sufficient to promote melanoma formation and invasion. *Mol Cancer* **12**, 117 (2013).
68. Rodriguez, M., Aladowicz, E., Lanfrancone, L. & Goding, C.R. Tbx3 represses E-cadherin expression and enhances melanoma invasiveness. *Cancer Res* **68**, 7872-81 (2008).
69. Han, J. et al. Tbx3 improves the germ-line competency of induced pluripotent stem cells. *Nature* **463**, 1096-100 (2010).
70. Ivanova, N. et al. Dissecting self-renewal in stem cells with RNA interference. *Nature* **442**, 533-8 (2006).
71. Stewart, S.A. et al. Lentivirus-delivered stable gene silencing by RNAi in primary cells. *RNA* **9**, 493-501 (2003).
72. Hong, H. et al. Suppression of induced pluripotent stem cell generation by the p53-p21 pathway. *Nature* **460**, 1132-5 (2009).
73. Elzi, D.J., Song, M., Hakala, K., Weintraub, S.T. & Shiio, Y. Wnt antagonist SFRP1 functions as a secreted mediator of senescence. *Mol Cell Biol* **32**, 4388-99 (2012).
74. Lessnick, S.L., Dacwag, C.S. & Golub, T.R. The Ewing's sarcoma oncoprotein EWS/FLI induces a p53-dependent growth arrest in primary human fibroblasts. *Cancer Cell* **1**, 393-401 (2002).

Figure Legends

TBX3, CAPERα = human; Tbx3, Caperα = mouse

Figure 1. CAPERα and TBX3 directly interact via the TBX3 repressor domain.

A) Representative spectrum for CAPERα identified in anti-TBX3 co-IP of HEK293 cell lysates. Mass spec analysis identified 6 specific CAPERα peptides, providing 8.5%

sequence coverage of the protein. This spectrum shows fragmentation of one of these peptides, C*PSIAAAIAAVNALHGR, with diagnostic b- and y-series ions shown in red and blue, respectively. * indicates carbamidomethylation

B) Anti-CAPERα immunoblot (IB) analysis of anti- CAPERα immunoprecipitated (IP'd, lane 2) e10.5 mouse embryo lysates.

Black arrowheads indicate IgG heavy chain and red indicate protein of interest (CAPERα or TBX3).

C) Anti-Tbx3 IB of anti-Tbx3 (lane 4) and anti-Caperα (lane 5) IP'd mouse embryo lysates.

Rabbit (r)-IgG (lanes1, 6) and mouse (m)-IgG (lane 7) are negative controls

D) *In vitro* MBP pull down assay: MBP and MBP-Tbx3 bound amylose affinity columns were incubated with GST or GST-CAPERα. Bound proteins were eluted, subjected to SDS-PAGE followed by IB with anti-CAPERα antibody.

E-G) Colocalization of Tbx3 and Caperα *in vivo* shown by immunohistochemical analysis of sectioned e10.5 mouse embryo: embryonic dorsal root ganglion (DRG, E), proximal (F) and distal (G) limb bud with anti-Tbx3 (red) and anti- Caperα (green) antibodies and DAPI (blue). White arrowheads in G label representative ectodermal and mesenchymal cells with cytoplasmic Tbx3 and nuclear Caperα.

H) Schematic representation of mouse Tbx3 overexpression constructs.Tbx3 DNA binding domain (DBD) point, ΔRD and exon7 missense proteins are untagged and the C-terminal deletion mutants are Myc-tagged.

I) Anti-TBX3 IB of HEK293 cell lysates transfected with control or anti-TBX3 shRNA.

J) Anti-CAPERα IB of anti-CAPERα IP'd samples from HEK293 cells transfected with anti-TBX3 shRNA and expressing mouse Tbx3 proteins listed at top. Production and IP of endogenous CAPERα is not affected by production of mutant Tbx3 proteins.

J') Anti-Tbx3 IB of anti-CAPERα IP'd samples from HEK293 cells transfected with anti-TBX3 shRNA and expressing Tbx3 proteins as in J. The DBD point mutant proteins (lanes 2,3) interact with CAPERα as efficiently as wild type Tbx3 (lanes 1, 4).
K) Anti-Myc IB of anti-Myc IP'd samples from HEK293 cell lysates expressing Myc-tagged mouse Tbx3 C-terminal deletion mutants. The mutant proteins are expressed and efficiently IP'd. These cells were not treated with anti-TBX3 shRNA because the expression constructs produce a Myc- tagged mutants that can be IP'd independently of endogenous TBX3.

K') anti-CAPERα IB of anti-Myc IP'd samples from HEK293 cell lysates expressing Myc-tagged mouse Tbx3 C-terminal deletion mutants. These cells were not treated with anti-TBX3 shRNA because the expression constructs produce a Myc- tagged mutants that can be IP'd independently of endogenous TBX3.

L) Anti-Tbx3 IB of anti-Tbx3 IP'd samples from HEK293 cells transfected with anti-TBX3 shRNA and expressing wt or repressor domain deletion mutant (ΔRD) mouseTbx3. The shRNA does not prevent production of the overexpression proteins.

L') Anti-CAPERα IB of HEK293 cells transfected with anti-TBX3 shRNA and expressing mouse wt or ΔRD Tbx3 proteins and IP'd with anti-Tbx3 or IgG. Loss of the repressor domain prevents interaction with CAPERα.

Black arrowheads indicate IgG heavy chain and red indicate protein of interest (CAPERα or TBX3).

Figure 1, Figure Supplement 1. Missense mutation of the C-terminus of Tbx3 disrupts interaction with CAPER α.
A) Anti-Tbx3 IB of exon 7 missense (ex7) and wt proteins expressed in HEK293 cells also transfected with anti-TBX3 shRNA. The overexpressed proteins are produced (red arrowhead).

B) anti-CAPERα and anti-TBX3 (C) IB of anti-CAPERα and negative control IP'd samples from HEK293 cells transfected with anti-TBX3 shRNA and overexpressing ex7

missense or wt Tbx3. Production and IP of endogenous CAPERα is not affected by production of mutant Tbx3 proteins.

C) Anti-Tbx3 IB of anti-CAPERα and negative control IP'd samples from HEK293 cells transfected with anti-TBX3 shRNA and overexpressing ex7 missense or wt Tbx3. The missense mutation disrupts interaction between Tbx3 and CAPERα.

Black arrowheads indicate IgG heavy chain and red indicate protein of interest (CAPERα or TBX3).

Figure 2. Knockdown of endogenous *CAPERα* and *TBX3* in primary human fibroblasts and mouse embryos induces premature senescence and disrupts expression of cell cycle and senescence regulators.

A-C) Representative bright field images of senescence associated β-galactosidase (SA-βG) assays of HFFs transduced with control, *TBX3* shRNA A or CAPERα shRNA A. Only occasional cells in the control transduction have detectable lacZ staining (blue) whereas knockdown of either TBX3 or CAPERα results in marked changes in cell morphology and increased lacZ staining.

D) Bar graph quantitating % beta-galactosidase positive cells from 4 replicate plates of SA-βgal assays. * indicates $p<0.001$ compared to control

E, F) 3T5 cell proliferation assay [74] of cumulative population doublings in HFFs transduced at passage 30 with control, TBX3 or CAPERα shRNAs. These are representative curves of duplicate experiments; each point on the curve is a measurement of cell count from a single plating followed over the course of the experiment as described in methods.

G-J) Immunohistochemical analysis of H3K9me3 immunoreactivity (red) and DAPI (blue) in HFFs after knockdown with control (G,I), TBX3 (H), or *CAPERα* (J) shRNAs.

Individual channels are shown and the merged image is on the right. Note increased nuclear punctate staining consistent with Senescence –associated heterochromatin foci (SAHFs) in both channels and evidence of nuclear disruption (white arrowheads in red channel) after loss of either TBX3 or *CAPERα*

K-M) Analysis of cell cycle and senescence marker transcript levels in HFFs transduced with control, *TBX3* or *CAPERα* shRNAs.

K) Relative transcript levels assessed by quantitative real time-PCR (qPCR) of cDNA. Values reflect fold change in knockdown HFFs relative to control after normalization to *HPRT* levels. Note general pattern of expression changes are similar in TBX3 (blue) and CAPERα (red) knockdowns.

Data are plotted as fold change mean +/- standard deviation. * indicates $p<0.05$ relative to control.

L, M) Agarose gel of PCR amplicons of cDNAs reverse transcribed from TBX3 (L) or CAPERα (M) shRNA knockdown HFF RNA reveals similar decreases in cell cycle promoting genes CDK2 and 4 in TBX3 and CAPERα knockdowns and increased p21 levels.

N, O) SA-βgal assay of wild type and *Tbx3* null MEFS reveals that Tbx3 is required to prevent premature senescence of primary murine embryonic fibroblasts (MEFs)..

P) Quantitation of % beta-galactosidase positive cells from 5 replicate experiments exemplified in O, P. * indicates $p<0.01$.

Q) 3T5 cell proliferation assay of cumulative population doublings in wild type and *Tbx3* null MEFs. These are representative curves from duplicate experiments; each point on the curve is a measurement of cell count from a single plating followed over the course of the experiment as described in methods.

R) IBs to assay levels of cell cycle and senescence proteins in wild type and *Tbx3* null embryo lysates. Tubulin loading control is at top left (Tub). The changes at the protein

level correlate with those observed at the RNA level (K-M) and RB is hypophosphorylated on multiple serine residues consistent with increased p16 and decreased CDK activity.

Figure 2, Figure Supplement 1. Effective knockdown of endogenous CAPERα in primary human foreskin fibroblasts using viral shRNA transduction.

A) RT-PCR analysis of *CAPERα* and *HPRT* transcript levels in HFFs transduced with two different retroviruses producing anti-CAPERα shRNAs (CAP sh A and B) and control shRNA virus (Ctl sh). Red arrowhead indicates CAPERα specific amplicon.

B) RT-PCR analysis of *CAPERα* and *HPRT* transcript levels in HFFs transduced with retroviruses producing anti-CAPERα shRNA A and a *CAPERα* overexpression virus (CAP OE). Note rescue of *CAPERα* expression by overexpression virus.

C-G) SA-βGal assays of HFFs transduced with control or CAPERα shRNAs A or B and rescue by CAPERα overexpression.

H) Quantitation of SA-βGal assays in C-G. * indicates $p<0.01$ compared to control shRNA.

I) Western blot showing depletion of endogenous CAPER*α* protein by CAP shRNA A. Anti-tubulin IB is loading control. This CAPER*α* shRNA "A" was used for all subsequent CAPER*α* shRNA knockdown experiments.

Figure 2, Figure Supplement 2. Effective knockdown of endogenous TBX3 in primary human foreskin fibroblasts using viral shRNA transduction.

A) RT-PCR analysis of *TBX3* and *HPRT* transcript levels in primary human foreskin fibroblasts (HFFs) transduced with control (Ctl sh) or *TBX3* (TBX3 shA) shRNA retrovirus.

B) RT-PCR analysis of *TBX3* and *HPRT* transcript levels in primary human foreskin fibroblasts (HFFs) transduced with control (Ctl sh) or *TBX3* (TBX3 shB) shRNA retrovirus.

C-G) SA-βGal assays of HFFs transduced with control or TBX3 shRNAs A or B and rescue by Tbx3 overexpression.

H) Quantitation of SA-βGal assays in C-G. * indicates $p<0.01$ compared to control shRNA.

I) Western blot showing depletion of endogenous TBX3 protein by TBX3 shRNA A. Anti-tubulin IB is loading control.

This TBX3 shRNA "A" was used for all subsequent TBX3 shRNA knockdown experiments.

Figure 2, Figure Supplement 3. *Tbx3* null murine embryonic fibroblasts (MEFS) have altered lamin β1 localization, nuclear disruption and mislocalized Caperα.

A-B') Representative WT and *Tbx3* null MEFs cells stained for laminβ1 at passage (P) 4 (A, B) and P1 (A', B'); note nuclear distortion and rupture in senescing *Tbx3* null MEFs as early as P1.

C) Quantitation of % distorted nuclei in WT versus *Tbx3* null MEFs. * indicates $p<0.05$.

D-F') Immunohistochemistry for Caperα (green) and DNA (DAPI, blue) in control and *Tbx3* null MEFs at P1 (D, D') and P2 E-F'). In mutant cells, Caperα signal shifts to nucleus from cytoplasm at P1, and large intranuclear Caperα+ foci are present by P2.

G) qPCR quantitation of senescence marker genes in WT versus *Tbx3* null MEFs. Data are displayed as mean fold change +/- standard deviation relative to WT after normalization to HPRT levels. * indicates p<0.01. # indicates p<0.05.

Figure 3. RB and p16 mediate senescence after CAPERα/TBX3 loss of function and CAPERα/TBX3 regulates chromatin structure of *CDKN2A-p16*.

A-F) SA-βgal assays of HFFs stably transduced with control (Ctl) or p53 [23] or RB [24] shRNAs subsequently transduced with CAPERα or TBX3 shRNAs.

G) % Quantitation of A-F from 3 replicate experiments. * indicates p<0.05 relative to Control or p53 shRNAs.

H) Cell proliferation assayed by crystal violet incorporation (OD units) in HFFs treated as in A-F. * indicates p<0.001 relative to Ctl or p53 shRNAs.

I-L) SA-βgal assays of HFFs stably transduced with control or p16 [25] shRNAs subsequently transduced with CAPERα or -TBX3 shRNAs.

M) % Quantitation of I-L from 3 replicate experiments. * indicates p<0.05 relative to Ctl shRNA.

N) Cell proliferation assayed by crystal violet incorporation (OD units) in HFFs treated as in I-L. * indicates p<0.01 relative to Ctl shRNA.

O) ChIP-PCR with antibodies listed at top on 3 regions upstream of the *CDKN2A-p16* transcriptional start site (TSS); position relative to (TSS) is indicated in parentheses at left of panels. PCR of input material used for the ChIP is shown under “Input”. The shRNA transduced is listed above each lane (HFF Tx). TBX3 knockdown decreases binding of TBX3 (lanes 8) and CAPERα (lanes 11) to all three regions. CAPERα knockdown has minimal effect on TBX3 binding (lanes 9). Knockdown of either TBX3 or

CAPERα decreases the repressive chromatin mark H3K9me3 (lanes14, 15) and increases the activating chromatin mark H3K4me3 (lanes 17, 18).

Figure 3, Figure Supplement 1. Effective knockdown of p53, RB and p16 in HFFs.

A) RT-PCR analysis of p53, RB and p16 transcript levels relative to HPRT after shRNA mediated KD in HFFs. The shRNAs employed for these knockdowns were obtained from Addgene and have been previously employed by numerous investigators [23-25,72,73].

Figure 3, Figure Supplement 2. UCSC Genome Browser view of the *CDKN2A* locus and 5' regions screened for binding by CAPERα and TBX3

Seven regions tested upstream of *CDKN2A-p16* promoter by ChIP with anti-TBX3 and anti- CAPERα antibodies. Amplicons are numbered black boxes 1-7 "Your Seq" at top superimposed on window from UCSC genome browser. Chromatin states in various cell types based are noted by colored bars below. Of these 7 regions, 3 were bound by both TBX3 and CAPERα: regions 3, 4 and 5 (data are presented in Fig. 3, panel O).

Figure 3, Figure Supplement 3.*CDKN2a-p16* H3K27 trimethylation markedly decreases in HFFS after knockdown of CAPERα or TBX3 consistent with activation of *CDKN2a-p16* expression.

ChIP-PCR of *CDKN2A-p16* regulatory elements with anti-H3K27me3 in control, TBX3 or CAPERα shRNA transduced HFFs. Locations of amplicons relative to transcription start site are noted in parentheses below each panel and correspond to regions 3, 4 and 5 in Fig. 3, Fig. Supplement 2.

Figure 3, Figure Supplement 4. Testing CAPERα and TBX3 binding to *p14, p21, CDK2, CDK4* and *CDKN1B* regulatory elements.

A) ChIP-PCR of *CDKN2A-p14* promoter with antibodies listed at top in control (C) and TBX3 siRNA (C') transduced HFFs. Red arrowhead indicates loss of CAPERα binding after TBX3 knockdown.

B-E) ChIP/PCR of HFF chromatin showing lack of TBX3 and CAPERα binding to known regulatory elements [29-31] of:

B) *CDKN1A-p21* (location relative to transcription start site is noted in parentheses at the bottom of the panels)

C) *CDK4*

D) *CDK2*

E) *CDKN1B*

Figure 4. CAPERα/TBX3 directly represses expression of the long noncoding RNA *UCA1*.

A-C) Gel showing RT-PCR analysis of *TBX3, CAPERα* and *HPRT* expression in control, TBX3 and CAPERα siRNA transfected HEK293 cells. The siRNAs effectively decreased transcript levels of their targets.

D) Differential display: representative PAGE gel of cDNAs derived from random primed, RT-PCR'd mRNAs from CAPERα, TBX3 and control siRNA transfected HEK293 cells. Blue arrowheads denote upregulated transcripts subsequently identified by sequencing as *DUSP4* and *UCA1*.

E, F) qPCR analysis of *TBX3* and *CAPERα* transcript levels in control and *TBX3* or *CAPERα* shRNA transduced HFFs (repeat of experiment shown in Fig.2 FS1A and 2A).

G) RT-PCR analysis of *UCA1* and *HPRT* gene expression in control, *TBX3* or *CAPERα* shRNA transduced HFFs.

H) qPCR analysis of *UCA1* transcript levels in control, TBX3 or CAPERα shRNA transduced HFFs.Results confirm differential display result that KD of TBX3 or CAPERα results in increase in *UCA1* transcript levels.

I) Schematic representation of the *UCA1* locus with primer sets employed for ChIP-PCR amplification of denoted regions 5' of gene (A1, A2, A3).

J) Anti-TBX3 ChIP-PCR of regions of the *UCA1* promoter in HFFs; only A3 is ChIP'd by TBX3 (lane 18, red arrowhead).

K) Anti-CAPERα ChIP-PCR of regions of the *UCA1* promoter in HFFs; only A3 chromatin is ChIP'd (lane 18, red arrowhead).

L) ChIP-PCR analysis of *UCA1/*A3 chromatin from in HFFs transduced with control (C) or TBX3 (KD) shRNA; ChIP antibodies are listed at top. Note decreased CAPERα binding after TBX3 KD (lane 17, red arrowhead), gain of activating mark H3K4me3 and loss of repressive marks H3K9me3 and H3K27me3.

M) ChIP-PCR analysis of *UCA1/*A3 with antibodies listed at top of panel in HFFs transduced with control (C) or *CAPER*α shRNAs. Note continued TBX3 binding despite *CAPER*α KD (lane 11, red arrowhead) and changes in chromatin marks parallel those seen in with TBX3 KD in panel L.

Figure 4, Figure Supplement 1. Validation of differential display findings.

A) Additional representative differential display gels with transcripts unchanged or independently affected by knockdown of CAPERα or TBX3 in HEK293 cells.

B) RT-PCR validating differential display result of increased *DUSP4* transcripts (Fig. 4D) after CAPERα or TBX3 KD in HEK293 cells.

Figure 5. *UCA1* expression is sufficient to induce senescence and required for normal execution of Oncogene Induced Senescence.

A) *UCA1* and *HPRT* transcripts assessed by RT-PCR in control and *UCA1*-overexpressing HFFs.

B, C) Representative bright field images of SA-βgal assay of cultured HFFs transfected with control and *UCA1* overexpression plasmids.

D) % quantitation of SA-βgal cells from 5 replicates in control and *UCA1* overexpressing HFFs. * indicates $p<0.05$.

E, F) Immunohistochemical analysis reveals co-localization of H3K9me3 and DAPI in SAHFs in HFFs transfected with *UCA1* overexpression plasmid (F) but not control plasmid (E).

G) Cell count of control and *UCA1* overexpressing HFFs 3 days post transfection. Mean +/- SD of 3 plates are shown at each time point. * indicates $p<0.005$ relative to control

H) Crystal violet assay of cell growth in control and *UCA1* overexpressing HFFs transfected with 2 μg of expression or control vector and assayed daily for 3 days post-transfection. * indicates $p<0.01$ relative to control.

I) Crystal violet assay of HFFs cultured for 3 days after transfecting 0, 1, 2 or 4 μg of control or *UCA1* overexpression plasmid. * indicates $p<0.01$ relative to control.

J) Transcript levels assessed by qPCR; values reflect fold change in *UCA1*-overexpressing HFFs relative to control after normalization to *HPRT* levels. * indicates $p<0.05$ relative to control.

K) qPCR analysis of *UCA1* expression in untransduced, presenescent (PS) HFFs and HFFs transduced with constitutively active ^{G12V}RAS (RAS). * indicates $p<0.05$ relative to PS.

L) Efficient knockdown of *UCA1* transcripts in RAS HFFs with *UCA1* shRNA (quantitated in panel T).

M-P) SA-βgal assays of RAS HFFs transduced with either control or *UCA1* shRNA at 3 (M, O) and 5 (N, P) days post transduction.

Q) % quantitation of SA-βgal cells from 6 replicate experiment as represented in panels M-P.
* indicates p<0.001 relative to control.

R) % quantitation of Ki67+ cells from 3 replicates in control versus *UCA1* shRNA transduced RAS HFFs. * indicates p<0.001 relative to control.

S) RT-PCR for *UCA1* transcripts shows persistent knockdown of *UCA1* in RAS shRNA cells with increasing passage (P0-P2).

T) qPCR analysis of fold changes in transcript levels of cell cycle and senescence genes after *UCA1* shRNA knockdown in RAS HFFs. * indicates p<0.05 relative to control.

U) ChIP-PCR analysis of *UCA1* region A3 with antibodies listed at top in PS and RAS HFFs. Note gain of activating (H3K4me3, H3K9ace, H4K5ace) and loss of repressive marks (H3K9me3, H3K27me3) at the *UCA1* locus after oncogene- induced senescence by RAS.

Figure 5, Figure Supplement 1. Western blots showing changes in protein levels in response to *UCA1* overexpression in HFFs.

pcDNA3.1 are control transfected cells and UCA1 were transfected with *UCA1* expression plasmid in pcDNA3.1 (as in Fig. 5, panel A). Note increased p16 and p21 levels and hypophosphorylation of RB.

Figure 5, Figure Supplement 2. ChIP-PCR assay for H3K9 acetylation of known regulatory elements of prosenescence and cell cycle genes whose expression is dyregulated after *UCA1* overexpression.

Input, rabbit IgG negative control ChIP, and H3K9acetylation ChIP in control "C" or *UCA1* "U" transfected HFFs for gene regulatory regions as labeled at bottom (primer sequences listed in ChIP primers section of methods). P16 a and b refer to amplicons –(2457-2040) and –(3107-2710), respectively. No changes in H3K9ace levels were detected in response to *UCA1* overexpression, suggesting that altered chromatin structure and subsequent increased transcription are not the cause of observed changes in transcript levels detected with UCA1 overexpression and shown in Fig. 5J.

Figure 6. UCA1 stabilizes CDKN2A-p16 mRNA levels during senescence by sequestering hnRNP A1.

A) Graphs of transcript levels assayed by RT-qPCR in HFFs transfected with control (blue) or *UCA1* (red) expression plasmids and treated with Actinomycin D. Y axis shows % mRNA level relative to time zero and X axis shows time in hours assayed post treatment. The estimated half-lives ($t_{1/2}$) were obtained using linear regression; the best fit lines, their equations and R values are shown in Figure 6, FS1. * indicates $p<0.04$ for $p16^{INK}$ and $p<0.01$ for all others.

B) Assay of mRNA levels in HFFs transfected with control or hnRNPA1 siRNA and treated with Actinomycin D. Axes and $t_{1/2}$ calculations are as in panel A. * indicates $p<0.05$.

C-E) Agarose gels of RT-PCR products assessing levels of *CDKN2A-p16* (p16, panel C), *UCA1* (panel D) and negative control lncRNA *TUG1* (panel E) transcripts in PS and RAS HFFs treated as labeled at top and subjected to RIP with anti-hnRNPA1 antibody.

mIgG lanes are negative controls for RIP assays.

Gels from left to right show: PS versus RAS; control versus *UCA1* overexpression; control versus TBX3 or CAPERα knockdown; RAS versus RAS/*UCA1* knockdown.

C) Lane 7 (red arrowhead) shows loss of $p16^{INK}$ /hnRNP A1 interaction in RAS.
Lane 14 (red arrowhead) shows loss of $p16^{INK}$ /hnRNP A1 interaction with *UCA1* overexpression.
Lanes 23 and 24 show loss of $p16^{INK}$ /hnRNP A1 interaction after TBX3 or CAPERα knockdown.
Lane 27 shows that *UCA1* knockdown decreases the total amount of $p16^{INK}$ mRNA in RAS cells.
Lane 31 shows that *UCA1* knockdown increases $p16^{INK}$ mRNA/hnRNP A1 binding (red arrowhead) in RAS cells, even though there is less total $p16^{INK}$ (lane 27)

F) Panels show immunoblots to detect hnRNP A1 protein in input samples assayed in panels C-E. Lanes are numbered to correspond with panels above.

Figure 6, Figure Supplement 1. Graphs showing best fit lines, their equations and R values used to calculate estimated mRNA half-life values shown in Figure 6A.

Figure 6, Figure Supplement 2. Northern blot assay of $p16^{INK}$ mRNA levels in the absence and presence of *UCA1*.

A) Top panel shows Northern blot of HFF cells transfected with control plasmid pcDNA3.1 and treated with Actinomycin D for the times (hours) indicated at top.

A') The ethidum bromide stained gel prior to transfer is shown for loading control and RNA quality.

A") The signals obtained by probing for $p16^{INK}$ mRNA in A were subjected to densitometric quantitation. Note decrease in signal at 2 and 4 hours consistent with the decay/ $t_{1/2}$ obtained in Figure 6A.

B) Top panel shows Northern blot of HFF cells transfected with UCA1 expression plasmid and treated with Actinomycin D for the times (hours) indicated at top.

B') The ethidum bromide stained gel prior to transfer is shown for loading control and RNA quality.

B") The signals obtained by probing for *p16^{INK}* mRNA in B were subjected to densitometric quantitation. Note that *UCA1* expression results in minimal decrease in signal at 2 and 4 hours, consistent with *UCA1*–mediated mRNA stabilization observed in Figure 6A.

Figure 6, Figure Supplement 3. Graphs showing best fit lines, their equations and R values used to calculate estimated half-life values after hnRNP A1 siRNA knockdown shown in Figure 6B.

A) Western blot assaying hnRNP A1 protein levels in HFFs after transfection of control or anti-hnRNP A1 siRNA.
B) Graphs of best fit lines, equations and R values for half-lives shown in Figure 6B.

Figure 6, Figure Supplement 4. RNA Immunoprecipitation analysis of hnRNP A1 interactions with *Myc* and *p14ARF* mRNAs.

RIP-PCR of *MYC* and *CDKN2A-p14* mRNAs shows they are bound by hnRNP A1 but these interactions are unaffected by OIS/RAS, *UCA1* overexpression, or knockdown of TBX3 or CAPERα.

Figure 6, Figure Supplement 5. RIP-PCR of HFF lysates using antibodies listed at top. Only hnRNP A1 (A) and hnRNP D (B) bind *UCA1* lncRNA, while *TUG1* and *H19* lncRNAs are bound by other hnRNPs.

Figure 6, Figure Supplement 6. RIP-PCR indicates that *RB, p21* and *CDK6* mRNAs do not interact with hnRNP A1 in PS or RAS HFFs.

Figure 7. Disruption of the CAPERα/TBX3 repressor by OIS activates *CDKN2A-p16* and *UCA1* to trigger a senescence transcriptional response.

A) ChIP-PCR of regions upstream of the *CDKN2A-p16* transcriptional start site (position relative to TSS in parentheses) in PS and RAS HFFs; the -3706-3308 amplicon is a negative control. OIS disrupts binding of *p16* regulatory elements (initially identified in Fig. 3O) by TBX3 and CAPERα.

B) ChIP-PCR of *p16* -4855 element shown in A. Decreased TBX3 and CAPERα binding in RAS correlates with loss of repressive chromatin marks and gain of activating marks. Evaluation of chromatin marks on the other *CDKN2A-p16* CAPERα/TBX3- responsive regulatory elements is shown in Fig. 7, Fig. Supplement 1A.

C) IBs for TBX3, CAPERα and actin loading control show increased amount of both proteins in RAS compared to PS HFFs.

D) Anti-TBX3 and anti-CAPERα IBs of IP'd proteins from PS and RAS HFFs.

F-M) Immunocytochemical staining of PS (F, G, J, K) and RAS (H, I, L, M) HFFS for TBX3 (F, H), Hoechst (DNA; G, I), CAPERα (J, L). Panels K, M are merged Hoechst/CAPERα. Scale bar for all panels is sown at lower right of panel I.

N-O') Functional analyses of genome wide transcriptional profiles of TBX3 KD, CAPERα KD, and control HFFs. All comparisons were statistically significant with p values <<<<0.0001; see Data Source File 3 for hypergeometric test, as implemented in the R statistical language, used to test significance of the number of genes found to be co-regulated between samples.

N) Venn diagrams show highly significant number of CAPERα/TBX3 co-upregulated transcripts (446 total), especially in the GO biologic process (BP) category of transcriptional regulation (122 transcripts) as assayed with DAVID. Pie chart shows KEGG pathway analysis of co-regulated genes.

N') Venn diagram showing 48 CAPERα/TBX3 co-upregulated transcripts also upregulated by RAS/OIS [46], especially in BP categories of transcriptional

regulation and programmed cell (pc) death. qPCR validation of coregulated genes is in S. Fig. 6A. Pie chart shows KEGG pathway analysis of OIS dataset.

O, O') As in N, N' but for downregulated genes. Pie chart in O' shows KEGG pathway analysis of OIS dataset; note most pathways are the same as in TBX3/CAPERα.

P, Q) Models of CAPERα/TBX3 repressor and *UCA1* function in proliferating (PS) HFFs versus RAS HFFs. In PS cell nuclei, CAPERα/TBX3 represses *UCA1, p16, p14* and *DUSP4* promoters in heterochromatin which permits ongoing cell proliferation. RAS disrupts the CAPERα/TBX3 complex and CAPERα relocates to dense intranuclear foci. Pro-senescence genes including *UCA1* and *p16* are converted to euchromatin and their expression/products induce senescence. In the cytoplasm of PS cells, hnRNP A1 binds and destabilizes *p16* mRNA, but activation of *UCA1* expression in OIS allows *UCA1* to sequester hnRNP A1 and stabilize *p16* mRNA.

Figure 7, Figure Supplement 1. Repression of *CDKN2A-p16* and *DUSP4* by CAPERα/TBX3 correlates with chromatin architecture and is relieved during oncogene induced senescence.

A) ChIP-PCR to assess chromatin marks on *CDKN2A-p16* regulatory elements in PS and RAS HFFs; antibodies are listed at top.

B) ChIP-PCR of *DUSP4* promoter in PS and RAS HFFs; antibodies are listed at top. TBX3 and CAPERα bind the *DUSP4* promoter in PS (lanes 6, 8) but not RAS HFFs (lanes 7, 9), and their occupancy correlates with altered chromatin marks consistent with de-repression in OIS/RAS cells (lanes 10-15).

Figure 7, Figure Supplement 2. CAPERα relocalization due to oncogene induced senescence is independent of PML bodies.

Immunocytochemical assay for endogenous CAPERα (green), PML (red) and DNA (DAPI, blue) in PS and RAS HFFs.

Figure 7, Figure Supplement 3. Validation of RNA-Seq identified expression changes induced by CAPERα and TBX3 KD.

qPCR validation of a subset of transcripts with altered expression detected by genome wide RNA-Seq on cDNA prepared from CAPERα (red) and TBX3 (blue) KD, and RAS HFFs (green). Downregulated transcripts are listed at left, upregulated at right.

Figure 7, Figure Supplement 4. IL6 and HDAC9 are direct targets of CAPERα /TBX3.

ChIP-PCR with antibodies listed at top showing CAPERα/TBX3 directly binds *IL6* (and *HDAC9* control elements. Effects of TBX3 or CAPER KD on chromatin marks are shown compared with control KD.

ChIP-PCR examining CAPERα/TBX3 binding to *IL6* and *HDAC9* control elements in PS and RAS HFFs; loss of binding correlates with altered chromatin marks.

Figure 7, Source Data File 1. Differentially expressed genes after knockdown of CAPERα in HFFs detected by RNA-Seq.

Figure 7, Source File Data 2. Differentially expressed genes after knockdown of TBX3 in HFFs detected by RNA-Seq.

Figure 7, Source Data File 3. Determining the statistical significance of shared differentially expressed genes using the hypergeometric test, as implemented in the R statistical language (phyper).

Figure 1 Kumar

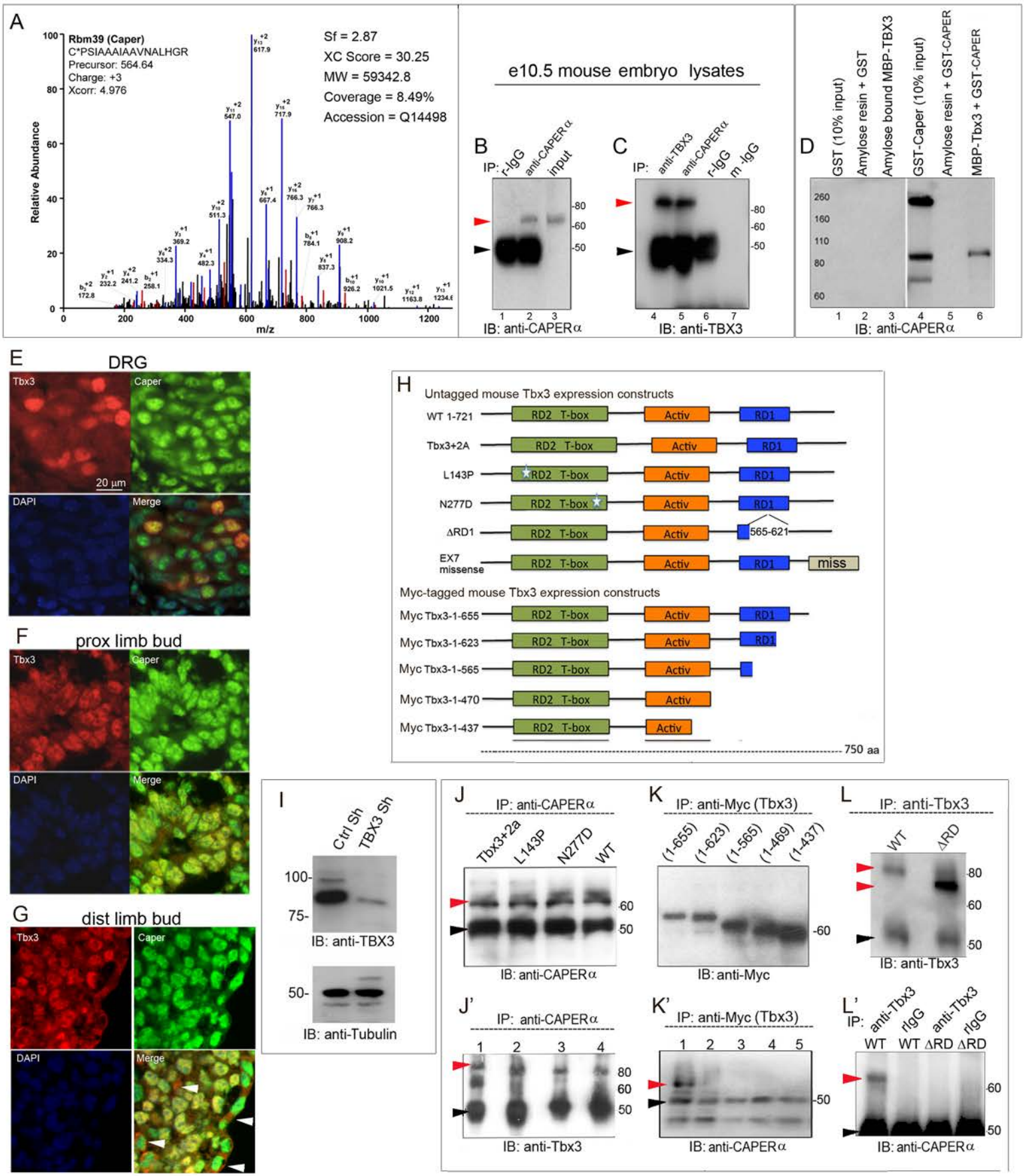

Figure 2 Kumar

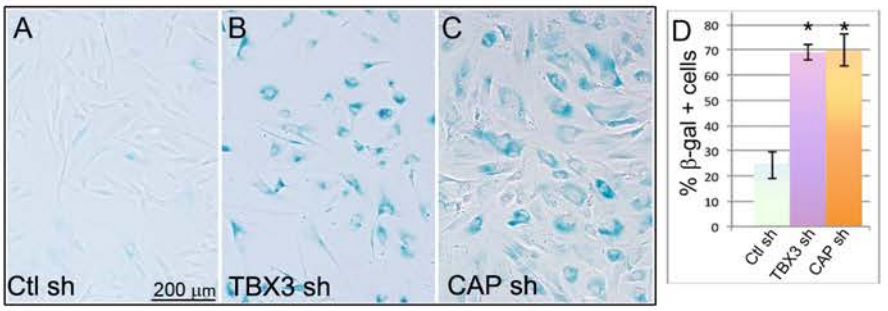

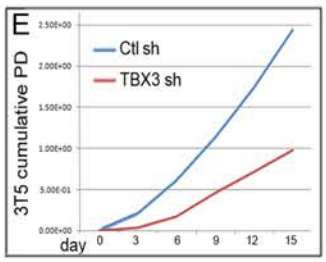

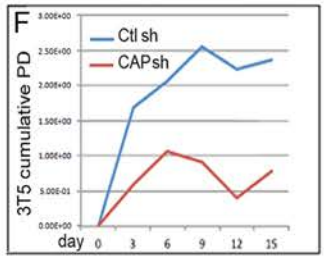

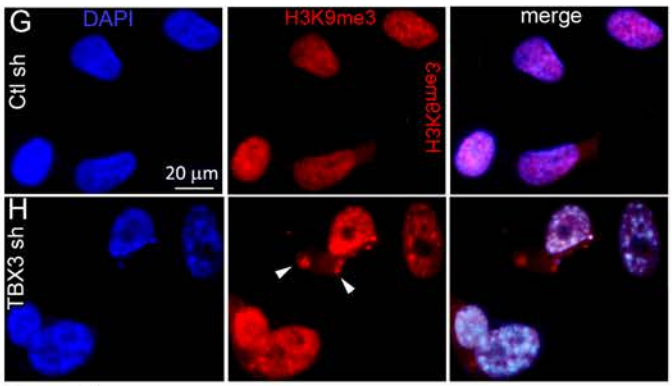

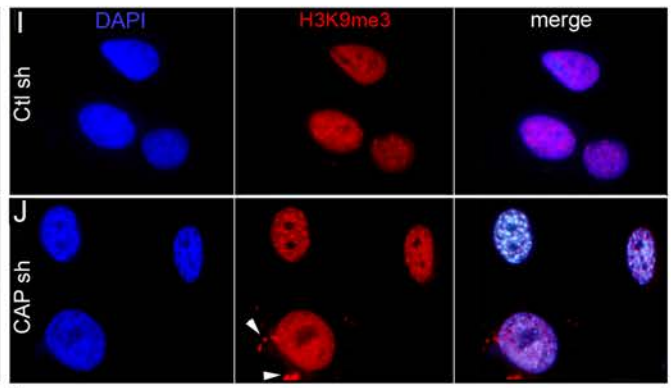

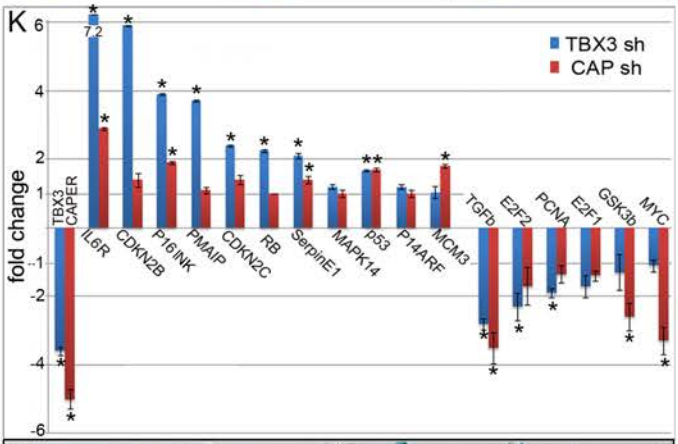

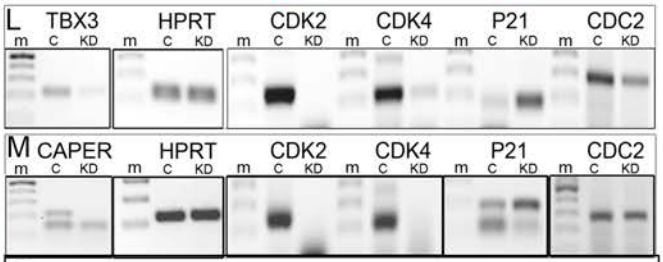

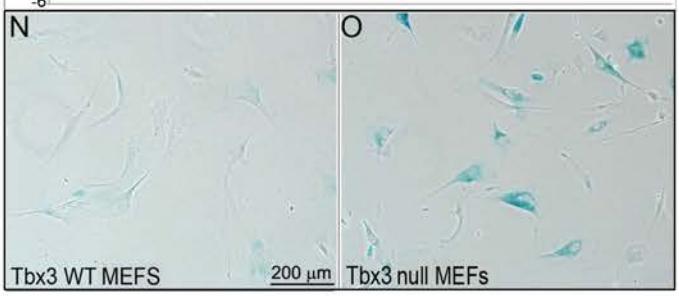

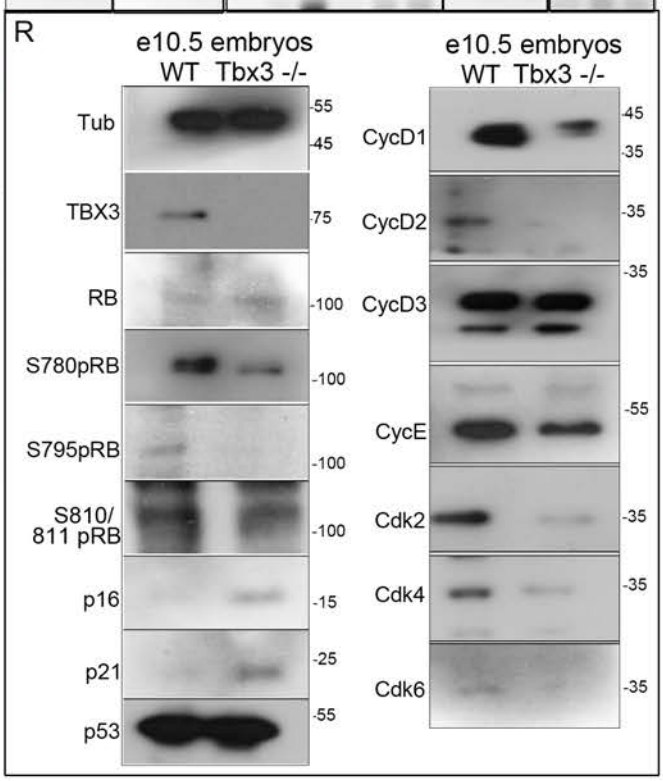

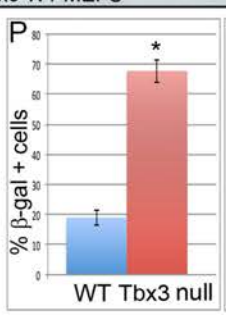

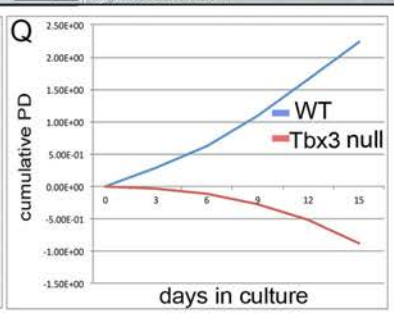

Figure 3 Kumar

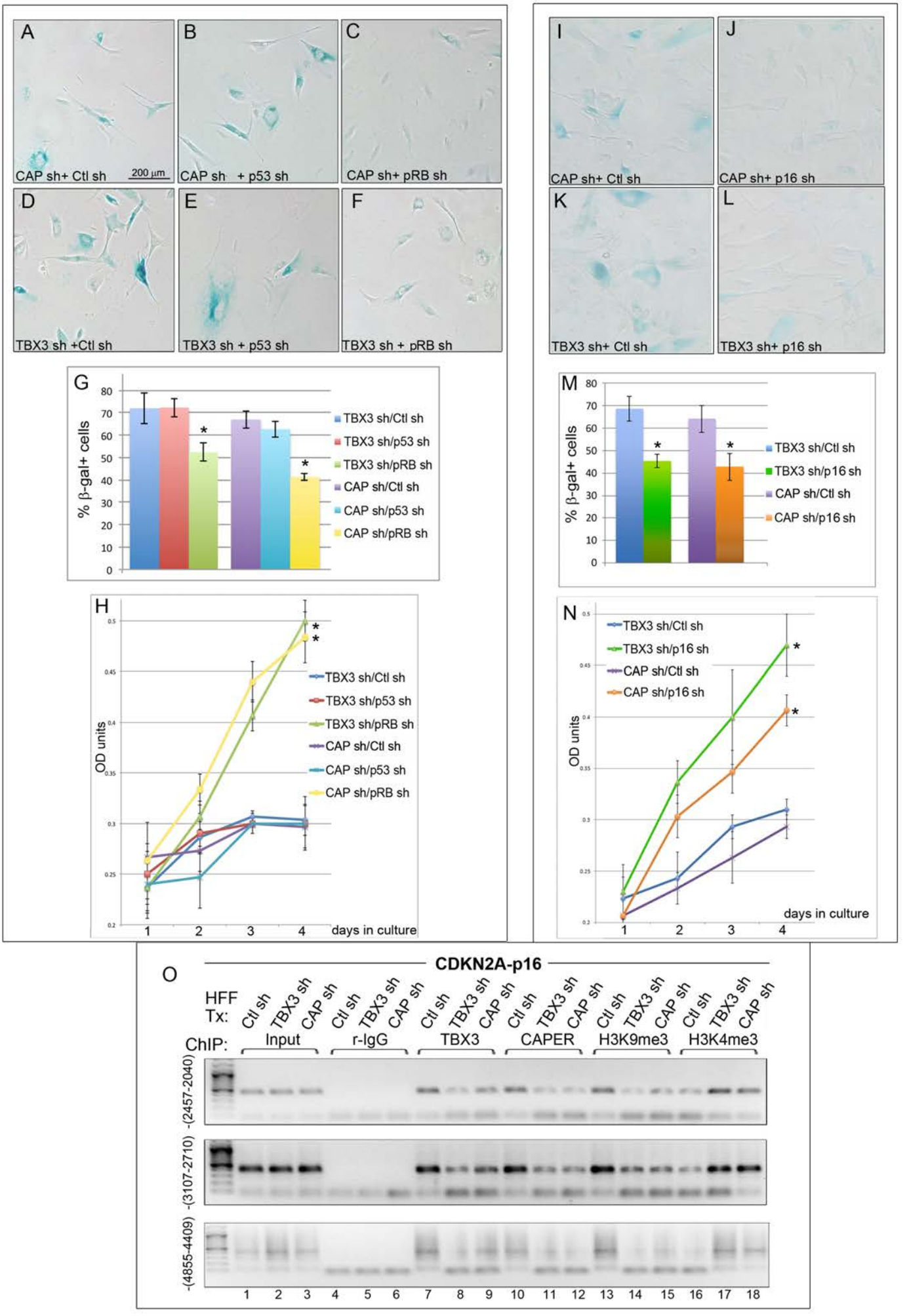

Figure 4 Kumar

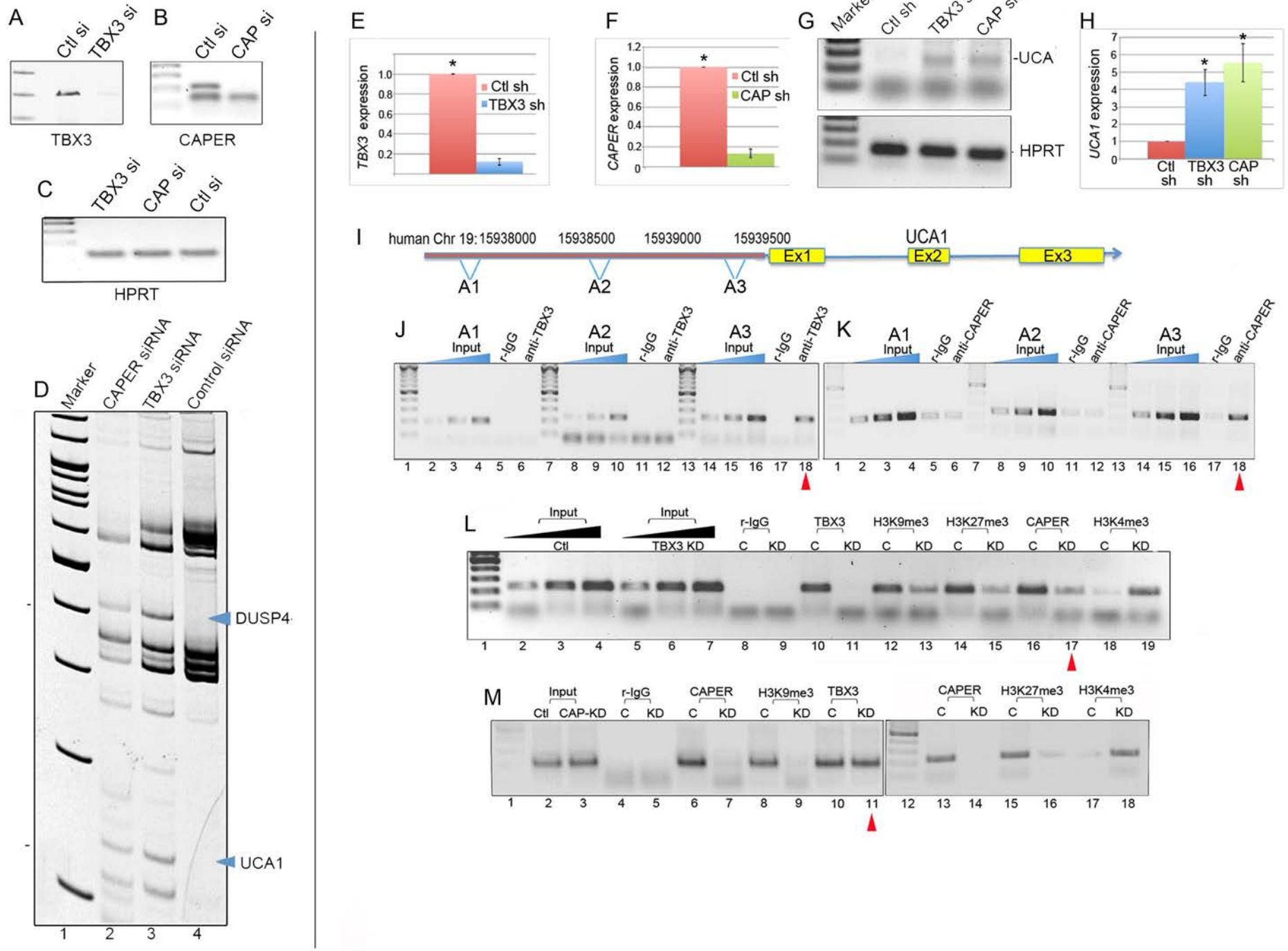

Figure 5 Kumar

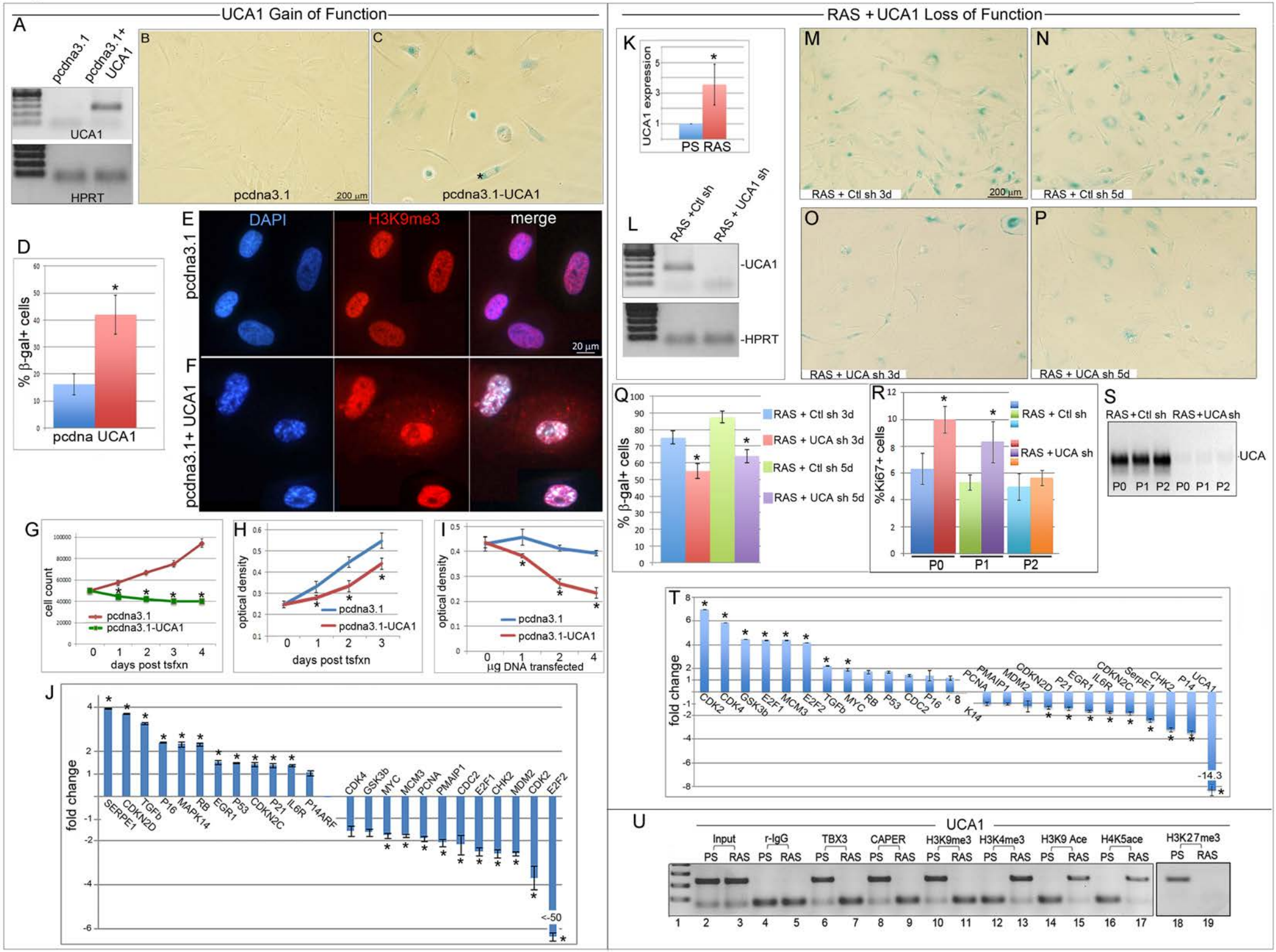

Figure 6 Kumar

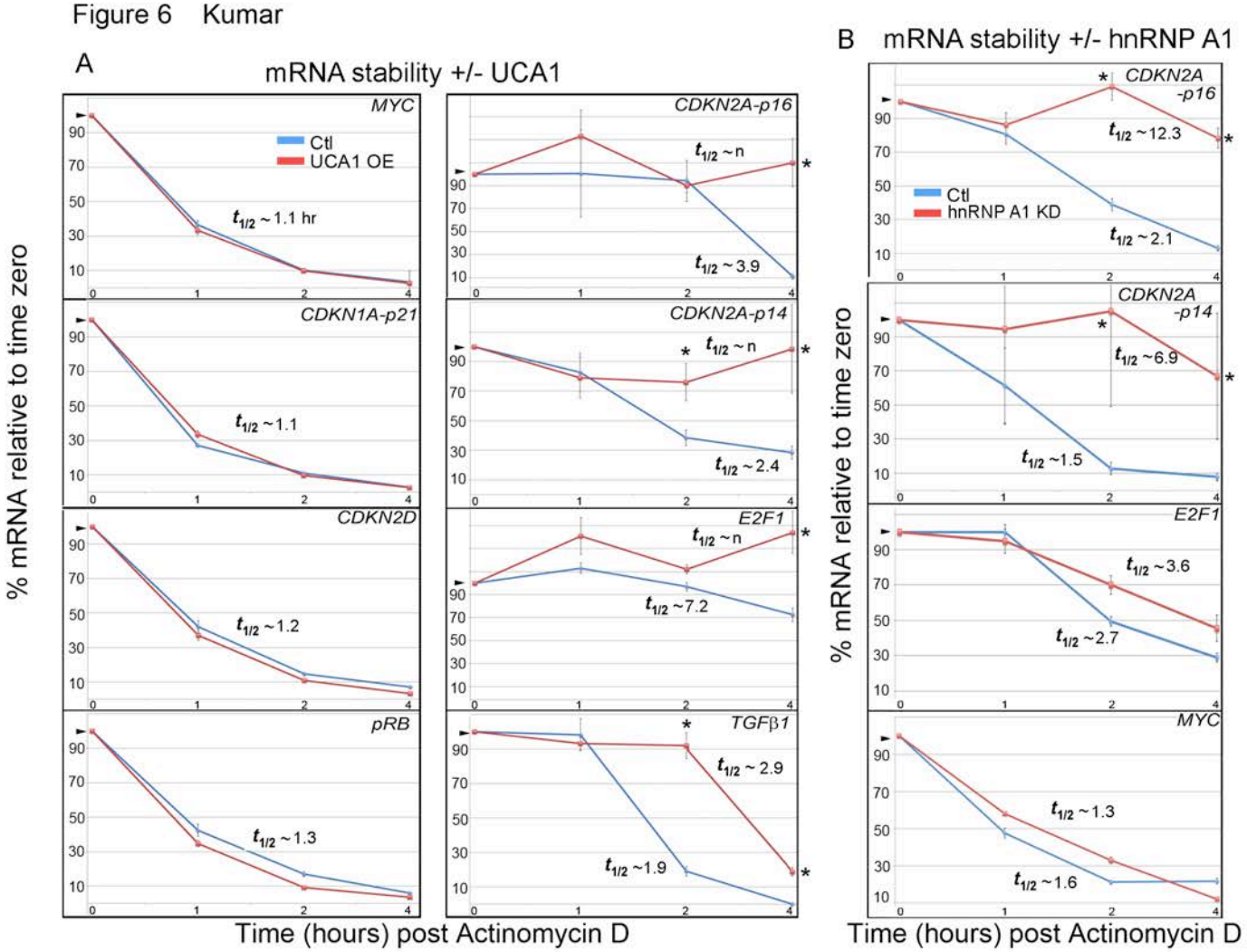

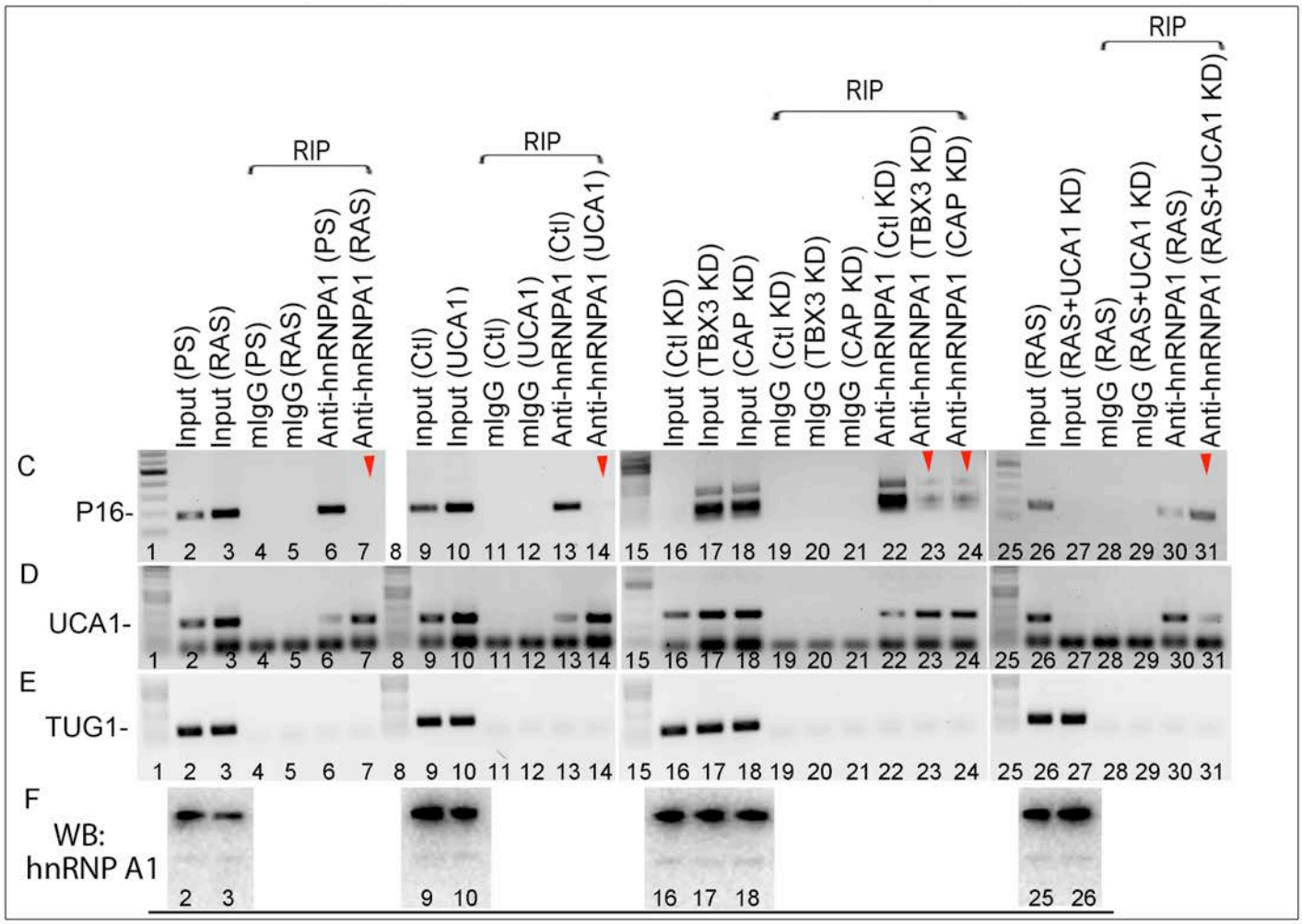

Figure 7 Kumar